Dist A

REPORT DOCUMENTATION PAGE

Form Approved

1. AGENCY USE ONLY (Leave blank)	2. REPORT DATE	3. REPORT TYPE AND DATES COVERED
		FINAL/23 SEP 91 TO 22 AUG 94

4. TITLE AND SUBTITLE

WAVELETS IN SIGNAL DETECTION AND IDENTIFICATION
COMPARATIVE SIGNAL PROCESSING TECHNOLOGY EVALUATION (U)

5. FUNDING NUMBERS

7933/DARPA
F49620-91-C-0097

6. AUTHOR(S)

Professor Raghu Raghaven

7. PERFORMING ORGANIZATION NAME(S) AND ADDRESS(ES)

Lockhead R&DD, D-9640/B-254
Lockheed Missiles & Space Co Inc
3251 Hanover Street
Palo Alto, CA 94303

8. PERFORMING ORGANIZATION REPORT NUMBER

AFOSR-TR-95-0098

9. SPONSORING/MONITORING AGENCY NAME(S) AND ADDRESS(ES)

AFOSR/NM
110 DUNCAN AVE, SUITE B115
BOLLING AFB DC 20332-0001

10. SPONSORING/MONITORING AGENCY REPORT NUMBER

F49620-91-C-0097

11. SUPPLEMENTARY NOTES

12a. DISTRIBUTION/AVAILABILITY STATEMENT

APPROVED FOR PUBLIC RELEASE: DISTRIBUTION IS UNLIMITED

A

12b. DISTRIBUTION CODE

UL

The Wavelet in Signal Detection and Identification: Comparative Signal Processing Technology Evaluation Program has been conducted by Lockheed Missiles & Space Company to develop wavelet based signal detection and classification techniques and compare them to Fourier time-frequency methods. The problem domain is submarine detection and identification using transient passive sonar signals. These nontraditional signals are critical in solving current Anti-Submarine Warfare (ASW) problems which include ultra quiet nuclear submarines and third world diesel submarines operating on batteries in shallow water. The Wavelets program supports the ARPA sponsored Multisensor Fusion System Program (MSF) at Lockheed (ARPA contract N00014-91-C-0237).

19950315 054

50

14. SECURITY CLASSIFICATION OF REPORT	15. SECURITY CLASSIFICATION OF THIS PAGE	16. SECURITY CLASSIFICATION OF ABSTRACT	17. LIMITATION OF ABSTRACT
UNCLASSIFIED	UNCLASSIFIED	UNCLASSIFIED	SAR(SAME AS REPORT)

TABLE OF CONTENTS

1. EXECUTIVE SUMMARY

The Wavelets in Signal Detection and Identification: Comparative Signal Processing Technology Evaluation Program has been conducted by Lockheed Missiles & Space Company to develop wavelet based signal detection and classification techniques and compare them to Fourier time-frequency methods. The problem domain is submarine detection and identification using transient passive sonar signals. These nontraditional signals are critical in solving current Anti-Submarine Warfare (ASW) problems which include ultra quiet nuclear submarines and third world diesel submarines operating on batteries in shallow water. The Wavelets program supports the ARPA sponsored Multisensor Fusion System Program (MSF) at Lockheed (ARPA contract N00014-91-C-0237).

The Wavelets program has the goal of performing comparative tests of wavelets and classical transform based techniques for signal detection and identification. The primary problem domain is processing underwater acoustic transients with the purpose of detecting and identifying submarines. Our overall approach to this problem is given in Figure 1.

A critical element in the program is the availability of well documented databases which are necessary for testing and validation. The data we have analyzed includes a large variety of synthetic, laboratory generated, biological and Navy transient databases. At the early stage of the program, we have implemented tools for generating chirps, tonals, gaussian weighted sinusoids, and sums of exponentially damped sinusoids. These synthetic signals were used for validating the performance of the various transforms. We have also generated an extensive set of acoustic transient signals in an office environment using a microphone designed for voice recording in conjunction with the acoustic digitizer. This in-house data set facilitated the validation of the end-to-end identification process. An introductory Navy biologics data set was acquired at the end of 1992, which included typical ocean noise such as whale cries, whale clicks, two type of porpoise cries, and shrimp clicks. This data set was used in our identification comparative tests. We have also processed a NUWC classified transient database consisting of a wide variety of signals obtained from diverse sensors in different environments. Finally, four classes of generic transients, namely impulsive, ringing, chirp, and noise-like transients, as described in the Navy Journal of Underwater Acoustics were generated and used extensively in our detection as well as identification comparative tests. More details on the databases are given in Section 2.

The transforms used in this study consists of two basic types: the Wavelet and the Fourier transforms. Within the Wavelet family, we have implemented the Daubechies Discrete Wavelet Transform (DWT), the Gauss-Morlet Continuous Wavelet Transform (CWT), and the M-Band Discrete Wavelet Transform. For the Fourier family, we have implemented the Short-Time Fourier Transform (STFT), the Gabor Transform, the Wigner-Ville Distribution (WVD), and the Choi-Williams Distribution (CWD). These transforms are described in Section 3.

Transient signals can be detected either in the time domain or in a transform domain. Under wideband ambient noise conditions, detection of a transient in the time domain may be inefficient especially if the transient signal has significant components on discrete elements of the transform space, i.e. frequency, signal shape. Therefore, we have concentrated our approaches to detection using STFT and DWT. The detectors were derived based on generalized likelihood ratio (GLR)

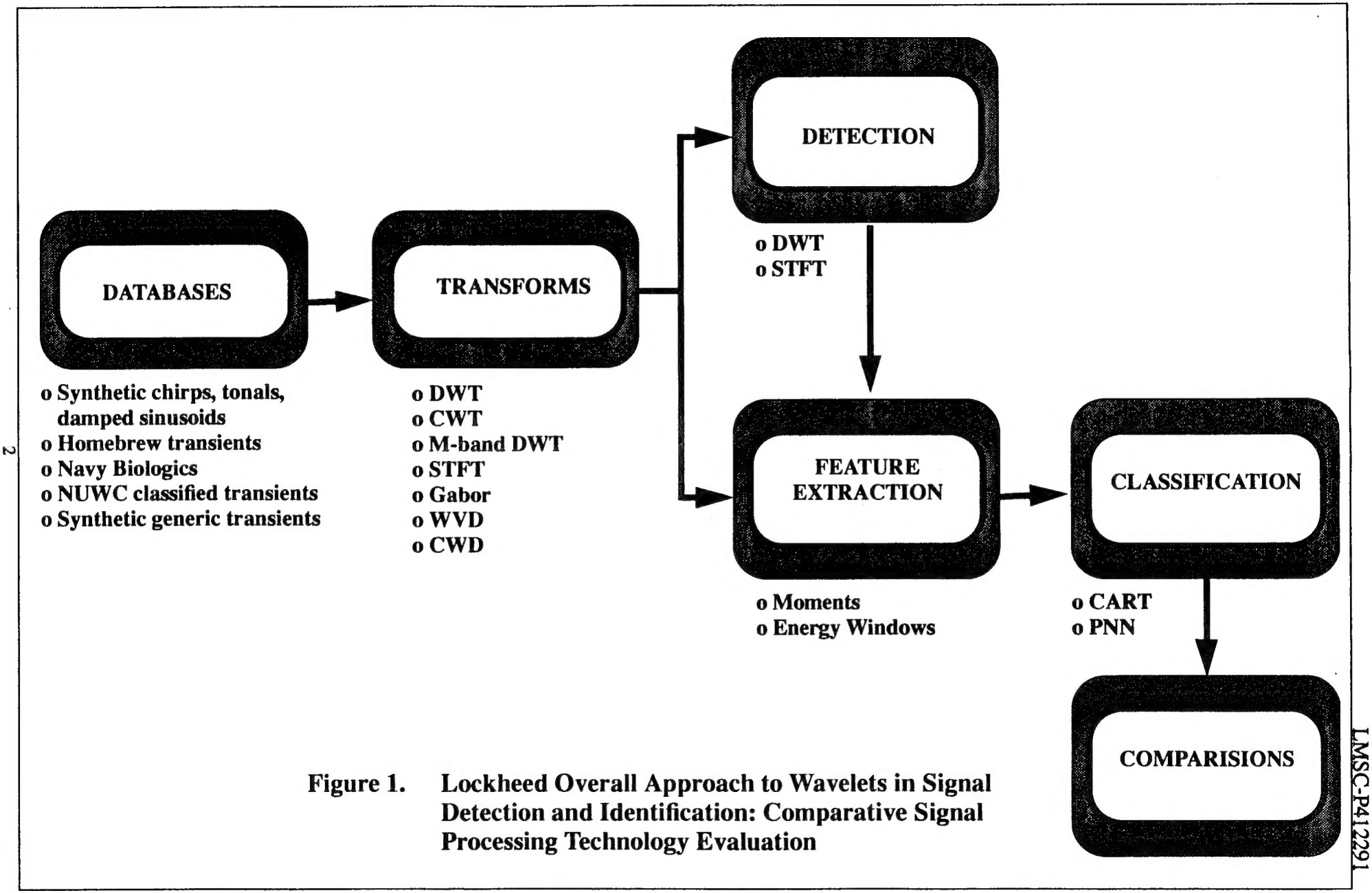

Figure 1. **Lockheed Overall Approach to Wavelets in Signal Detection and Identification: Comparative Signal Processing Technology Evaluation**

testing statistics for testing the null hypothesis where the received signal is noise only versus the alternative hypothesis where the received signal is noise plus real signal. A version of the WolcinWolcin sequential detector was used which produces a statistic consisting of the maximum likelihood signal power estimates in frequency and time. The derivations of both the STFT based generalized likelihood ratio detector and the DWT based generalized likelihood ratio detector are given in Section 4. Both detectors have been implemented and used extensively in the detection comparative tests.

The most critical item in signal identification is the extraction of features which describe the signal characteristics. These features must be robust, shift invariant and of low dimensionality. The Wavelet transform as opposed to the Fourier transform is extremely sensitive to shifts in the position of the signal relative to the processing window. This means that a one-sample time difference in signal detection results in completely different Wavelet transform coefficients. Considerable efforts were focused on developing shift invariant Wavelet features. Wavelet features were developed using moments and energy windows in the time-scale plane and parametric fits to the transform waveform. Time-frequency features were derived for the STFT and WVD using adaptive energy windows in the time-frequency plane and parametric fits to the transform waveform. Section 5 contains the details.

As for classification, the Classification And Regression Trees (CART) algorithm was our baseline classifier. It is a binary tree classifier which uses linear combinations of features and ranks the features in terms of discrimination power. Also employed in this study was a nonparametric classifier known as Probabilistic Neural Network (PNN). This classifier estimates the class density functions by Parzen windows. Both classifiers are discussed in Section 6 and were used in the comparative tests for transient signal identification.

Extensive comparative tests of Wavelet with Fourier transform based techniques for signal detection and identification have been completed using synthetic, laboratory generated, biological and Navy transient databases. The results we have obtained for detecting the arrival time of the transients indicated that the DWT detector does better than the STFT detector when the transients are wideband. When the signal is narrowband, however, STFT detector performs better than DWT. As for detecting the generic transients, the STFT detector consistently performs much better than the DWT detector for all four generic types. For ringing (Type II) and chirp transients (Type III) in particular, the STFT detector is nearly perfect in detecting the arrival time of the transient with its probability of detection (PD) extremely close to 1 and its probability of false alarum (PFA) extremely close to 0.

As for identification comparative tests, the analysis we have performed on Navy biologics data set indicated that if we use CWT with adaptive scaling on peak energy, CWT techniques outperform all of the STFT techniques. The NUWC classified transient databases contain classes that are made up of signals from different environments and a range of signal-to-noise ratios (SNR). Since the SNR is generally high and the between-class differences are large enough that these signals do not provide a rigorous comparison of the techniques. Both the CWT and STFT performed comparably in this case. We have conducted extensive identification comparative tests of the Wave Packet (WP) approach against the CWT based classifier and the STFT based classifier on the synthetic generic transient data sets. The between-class identification results indicated that when the SNR

is positive, all three approaches perform extremely well with the WP performing consistently better than the CWT and STFT. When the SNR is negative, the STFT outperforms the other two. In cases where the SNR is worse than -14 dB, all three approaches showed an error of more than 50%. The "within-class" identification results showed that the STFT outperforms the other two approaches in classifying the subclasses within the impulsive transient class. When the SNR is negative, all three approaches showed a "within-class" classification error of more than 50%. For identifying the subclasses within the ringing and chirp transient class, the CWT in general outperforms the STFT and WP based classification schemes. Again, when the SNR is worse than around -10 dB, all three approaches showed a "within-class" classification error of more than 50%. Section 7 contains, for each comparative test, a detailed description of the experiment, the results, and the findings.

The various detection and identification techniques developed under this Contract have been transferred to the MSF Program and are currently being validated as part of the MSF testbed. Also transferred is the Wavelets Quicklook Tool which permits random access of data in huge databases, extraction of signals of interest and classifying them based on both sound and transform characteristics. Screening and processing of MSF Sea Test data would not have been possible without our Wavelet Quicklook Tool. Several key features of this tool is given in Section 8.

A number of related activities performed under Lockheed Independent Research projects are reported in Section 9. Of particular interest is the parallel implementation of the continuous wavelet transform and its timing benchmarks.

The Wavelets program is a three year effort. This report summarizes the technical findings and accomplishments made during the Contract period: September 23, 1991 to September 22, 1994.

2. DATABASES

2.1. Synthetic Chirps, Tonals, Damped Sinusoids

Tools for generating chirps, tonals, gaussian weighted sinusoids, sums of exponentially damped sinusoids and synthetic biological sounds were implemented. These synthetic signals were used for validating the performance of the various transforms.

The equation for a chirp is given by:

$$chirp(\alpha, \beta, \omega_0) = Ae^{-\frac{\alpha t^2}{2} + \frac{i\beta t^2}{2} + i\omega_0 t}$$

where α is the damping factor
β is the oscillating factor and
ω_0 is the center frequency
A is the amplitude

Figures 2 to 5 show several chirp signals and their corresponding Short-Time Fourier Transforms.

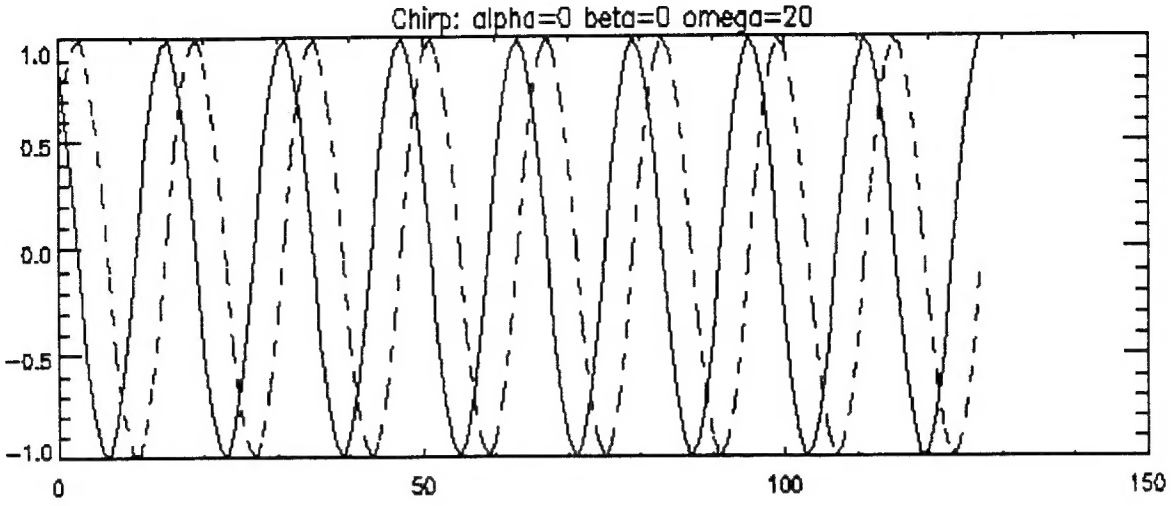

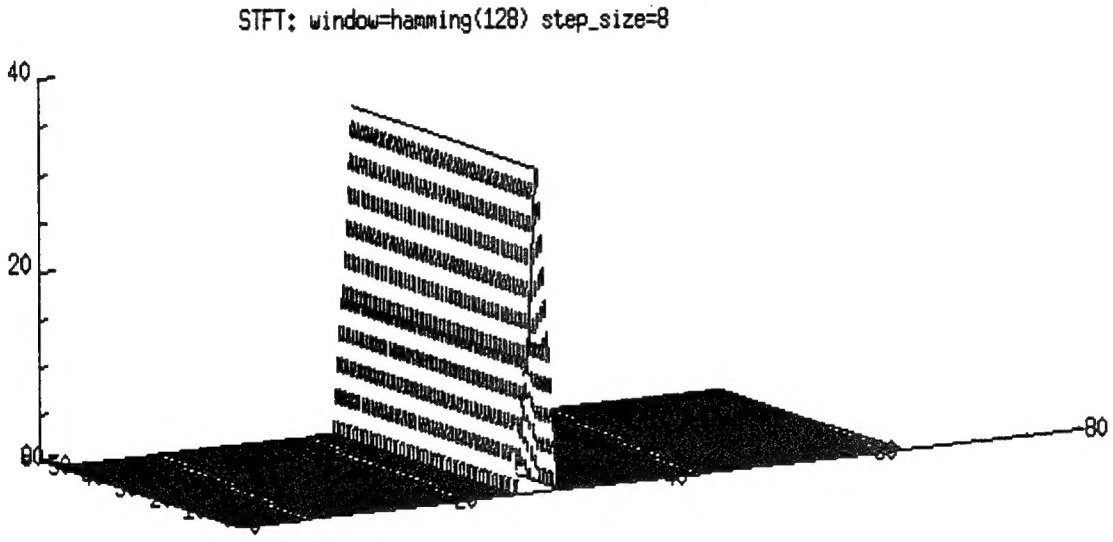

Figure 2. chirp(0,0,20) and its STFT

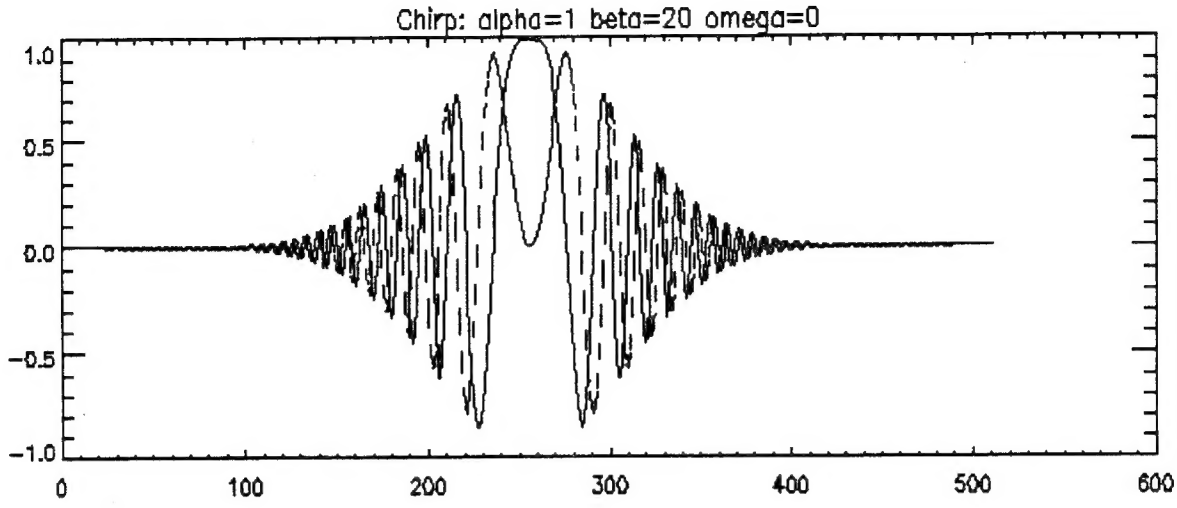

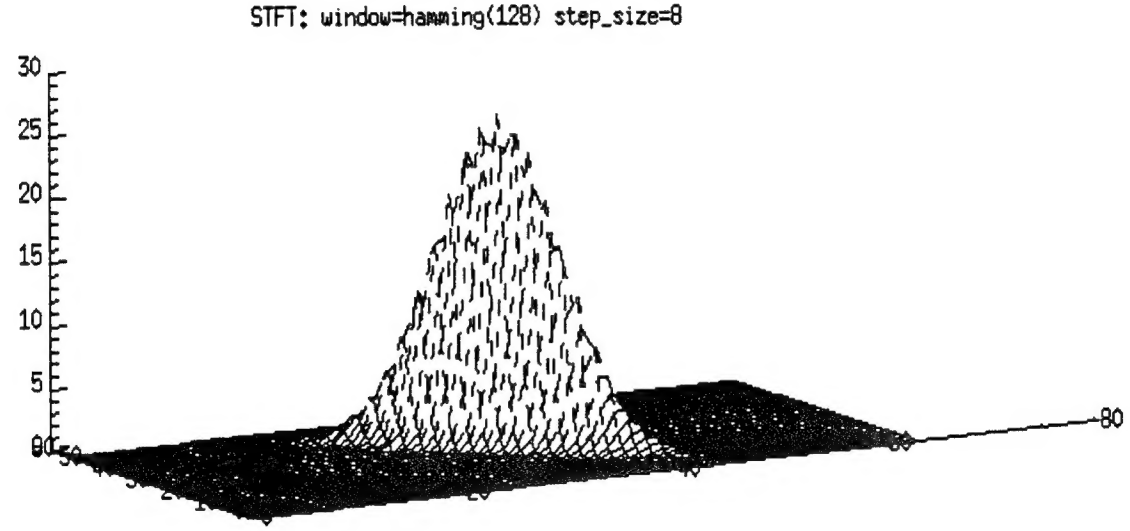

Figure 3. chirp(1,20,0) and its STFT

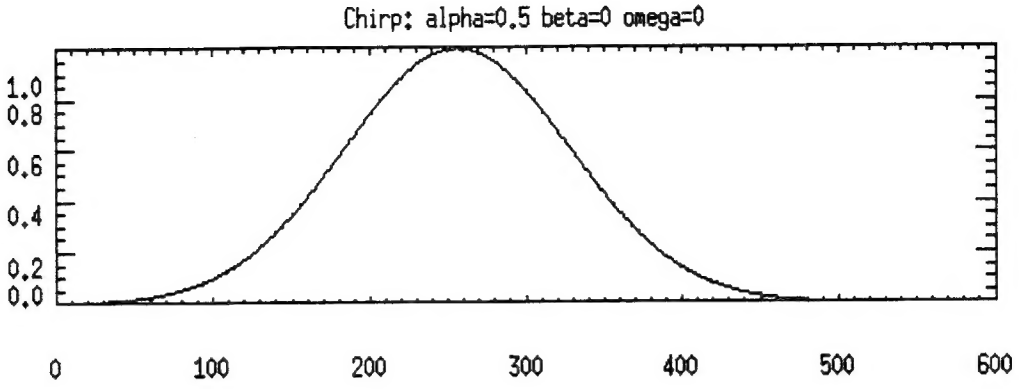

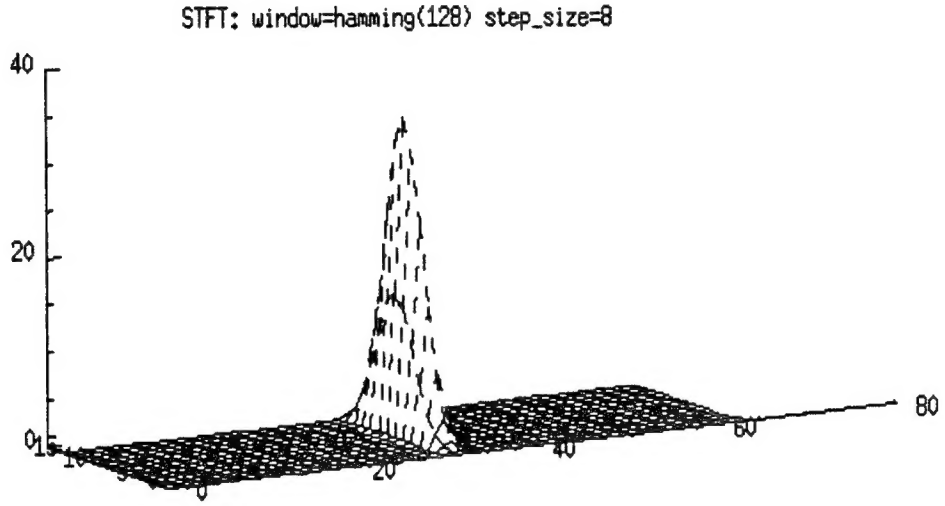

Figure 4. chirp(0.5,0,0) and its STFT

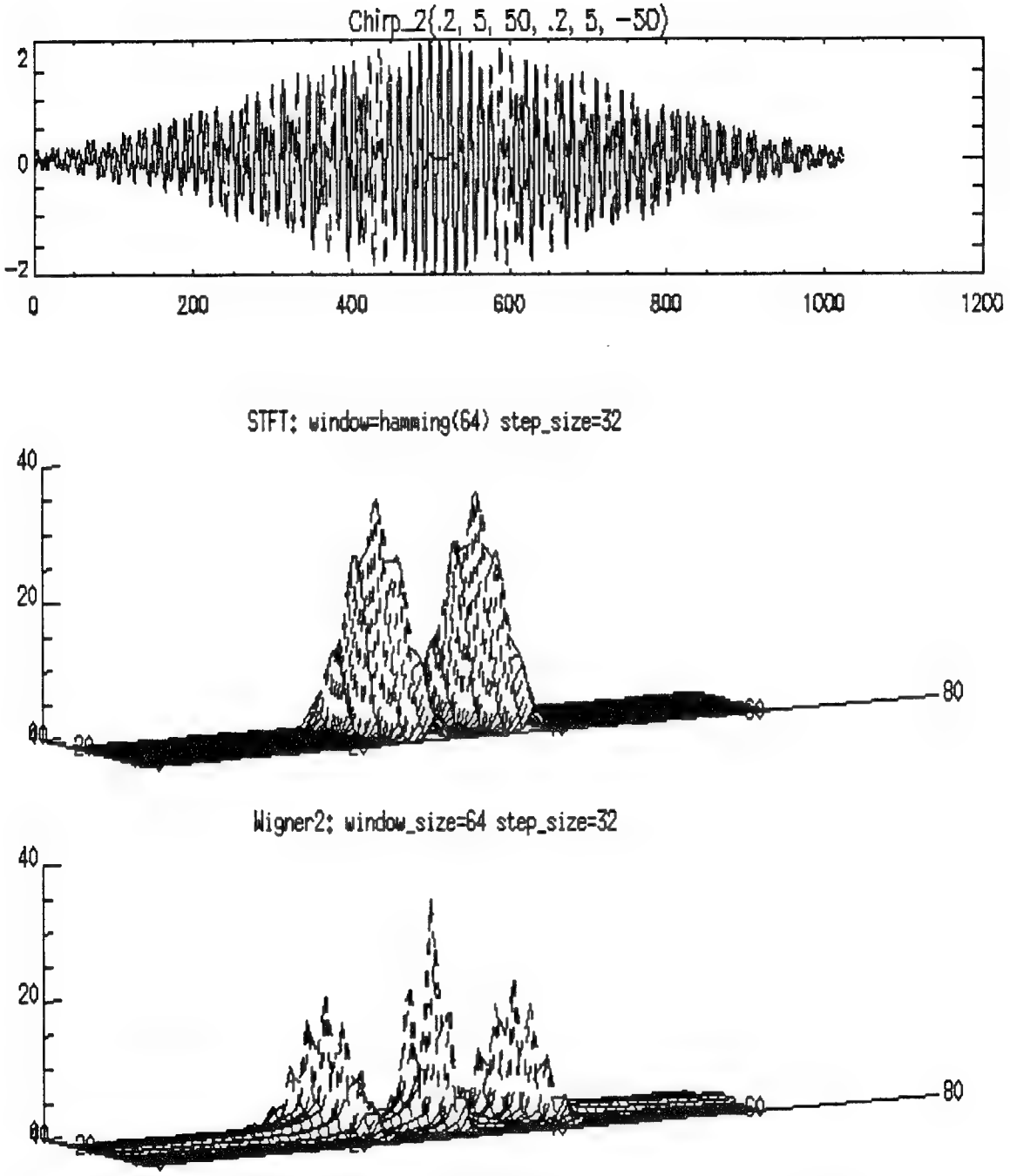

Figure 5. Sum of chirp(0.2,5,50) and chirp(0.2,5,-50), its STFT, and its WVD

The equation for the double sided damped cosine is

$$damped\cos ine\,(\alpha, \omega_0) = A\cos(\omega_0 t)\, e^{-\alpha t^2}$$

where α is the damping factor
ω_0 is the center frequency
A is the amplitude

Figure 6 shows a damped cosine signal, the damped cosine signal embedded in Gaussian noise, and the Gauss-Morlet Continuous Wavelet Transform of the damped cosine signal in Gaussian noise.

The technique for generating synthetic porpoise signals can be applied to a wide class of chirp like signals. The synthesis process involves three steps. The first step creates a frequency function $f(t)$. The frequency function employed is an exponentially damped sinusoid.

$$f(t) = (A\sin((2\pi Ct) + B)\, e^{-tD})$$

where A is the amplitude
B is the base frequency
C is the cycle
D is the decay rate

The second step uses this frequency function to modulate a sinusoid.

$$s(t) = \sin(2\pi t f(t))$$

The third step applies a volume envelope to the resulting function. The envelop function employed is the gamma function

$$g(t) = \frac{t^{(a-1)}\, e^{(-t/b)}}{(b^a (a-1)!)}$$

The equation for a porpoise signal is

$$porpoise\,(t) = s(t)\, g(t)$$

These synthetic porpoise signals are typical of ones in the NUWC database. Figure 7 shows the Short-Time Fourier Transform of a porpoise signal consisting of three components with different base frequencies B (880, 1496 and 2094 Hz) and amplitudes A (1000, 750, 562). The other parameters were cycles $C = 2$, decay rate $D = 4$, gamma parameters $a = 0.2$ and $b = 1$. The signal duration was 0.6 seconds.

2.2. Homebrew Transient Test Set

A variety of transient acoustic signals were generated in an office environment. A microphone

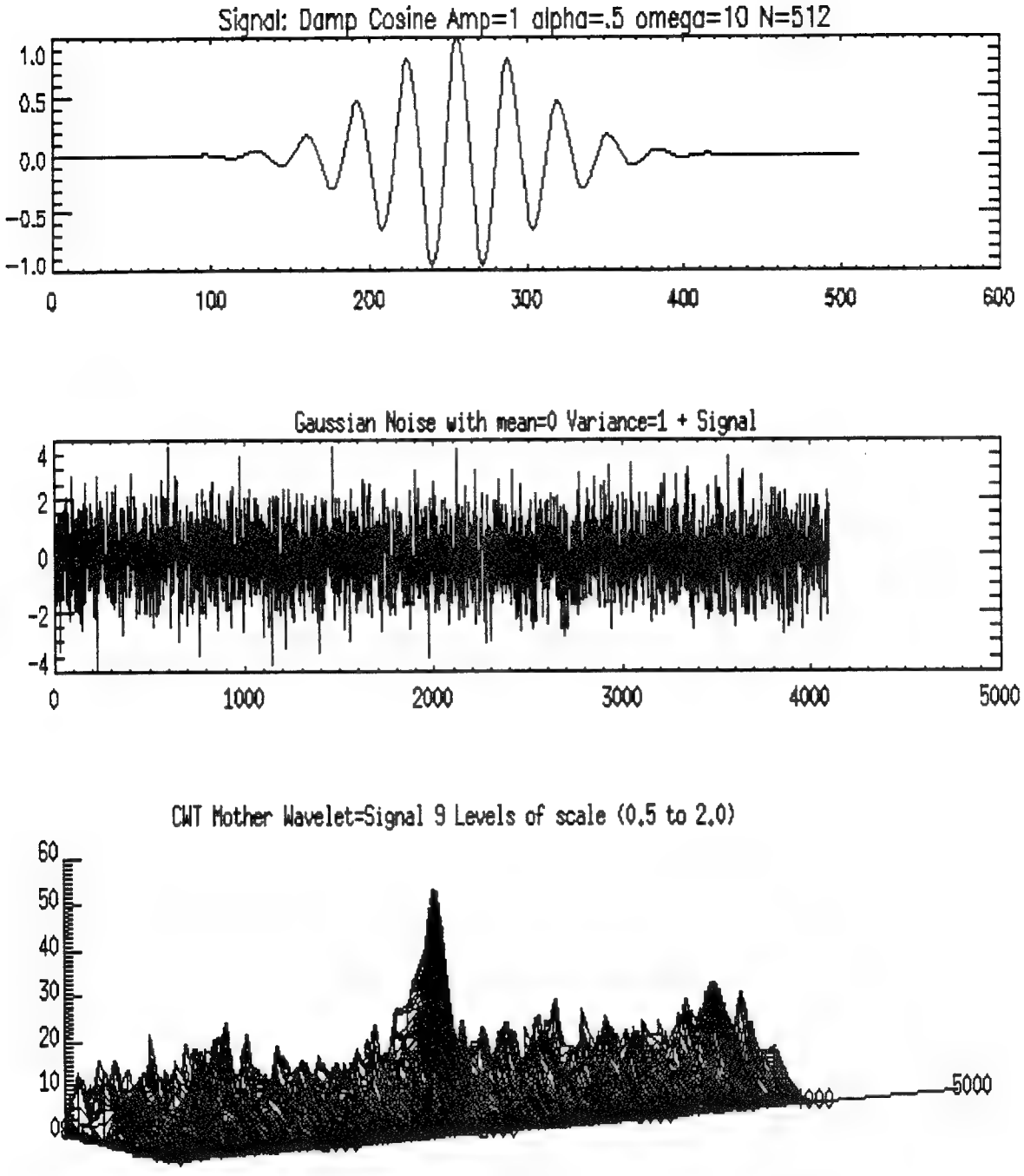

Figure 6. Damped Cosine, Damped Cosine in Gaussian Noise, and CWT of Damped Cosine in Gaussian Noise

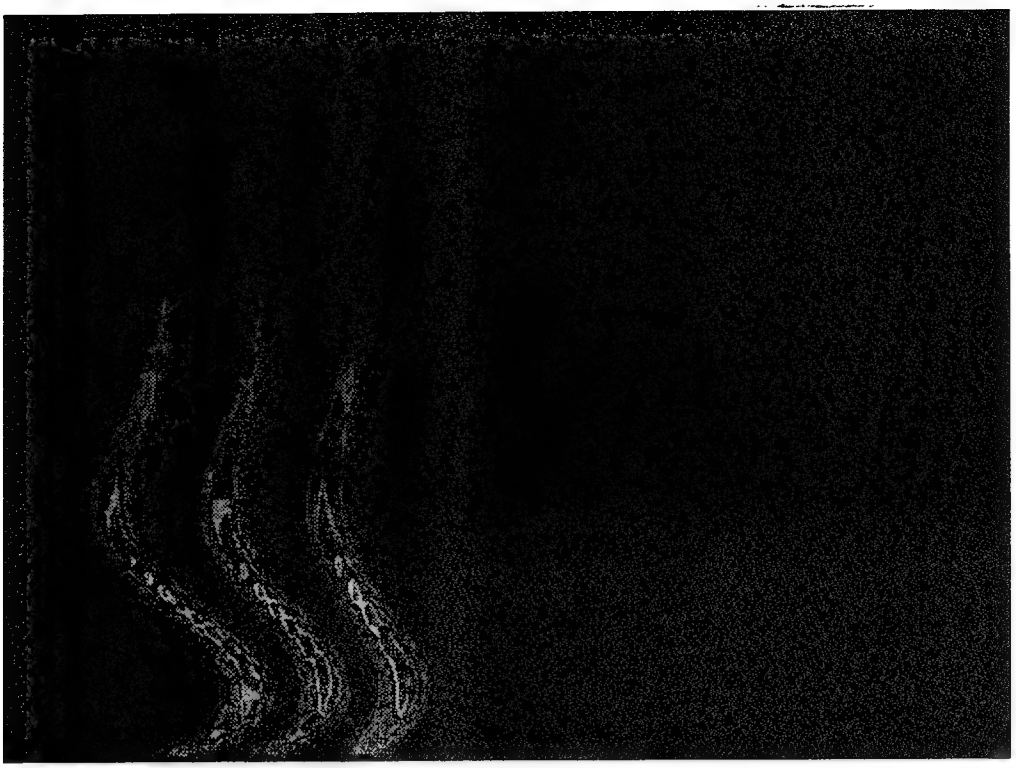

Figure 7. The STFT of a synthetic porpoise signal with three components. The vertical axis is time and horizontal is frequency.

designed for voice recording was used in conjunction with the acoustic digitizer in a SUN IPC workstation. The microphone used has a frequency response between 100 and 10,000 Hz. Although not ideal for capturing all of the information in a wideband transient signal, this microphone has better performance than is possible underwater where the media strongly attenuates frequencies over 1,000 Hz. The SUN 8-bit digitizer quantizes at 8000 samples per second. This is not as good as typical underwater systems which operate at 12 bits and 25,000 samples per second. 36 samples were generated for each of the 6 classes listed in Table 1 below.

Class	Description
Table	Fist pounded on computer table
Brick	Lead brick dropped on computer table
Squeak	Squeak produced by lock mechanism on file cabinet (Note this is almost a pure tone)
Drawer	Slammed drawer on desk
Door	Slammed door to office (Note this signal has two parts)
Clank	Two iron barbells slammed together

Table 1. Signal classes for in-house database

Figure 8 shows the time-amplitude plot of one example from each class. Considerable within class variation means that the examples shown are not necessarily "typical.".

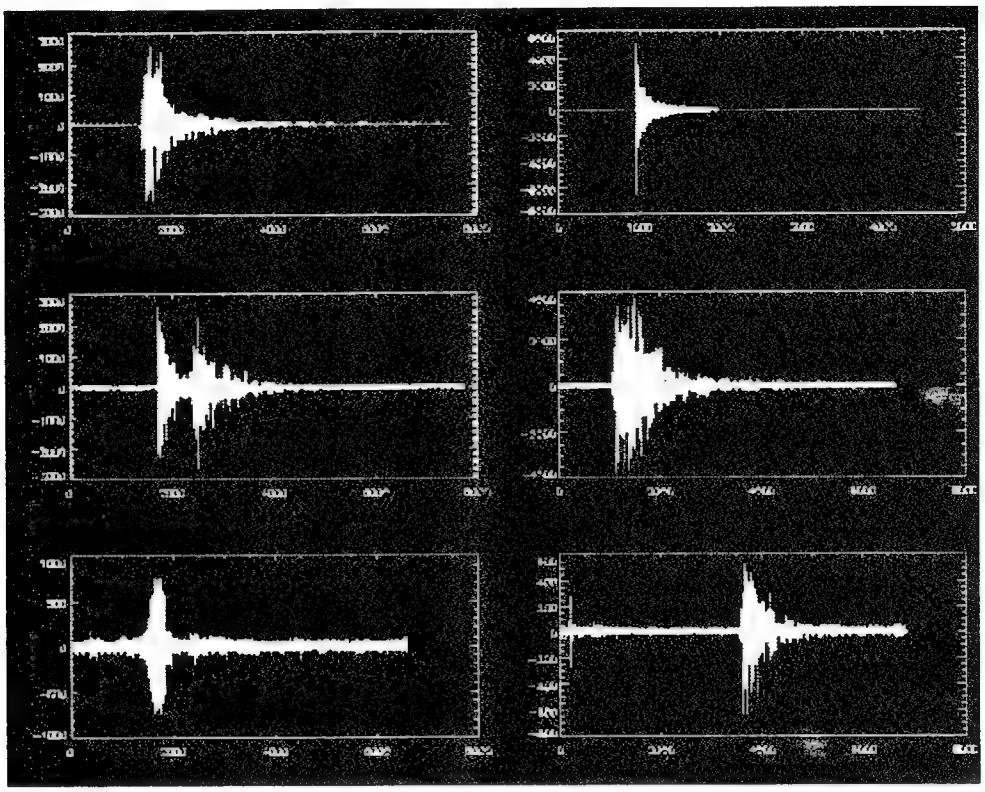

Figure 8. Time-amplitude history of one signal from each class.
Top row: table, clank. Middle row: door, drawer. Bottom row: squeak, brick.

Figure 9 shows the Fourier transform of one example from each class.

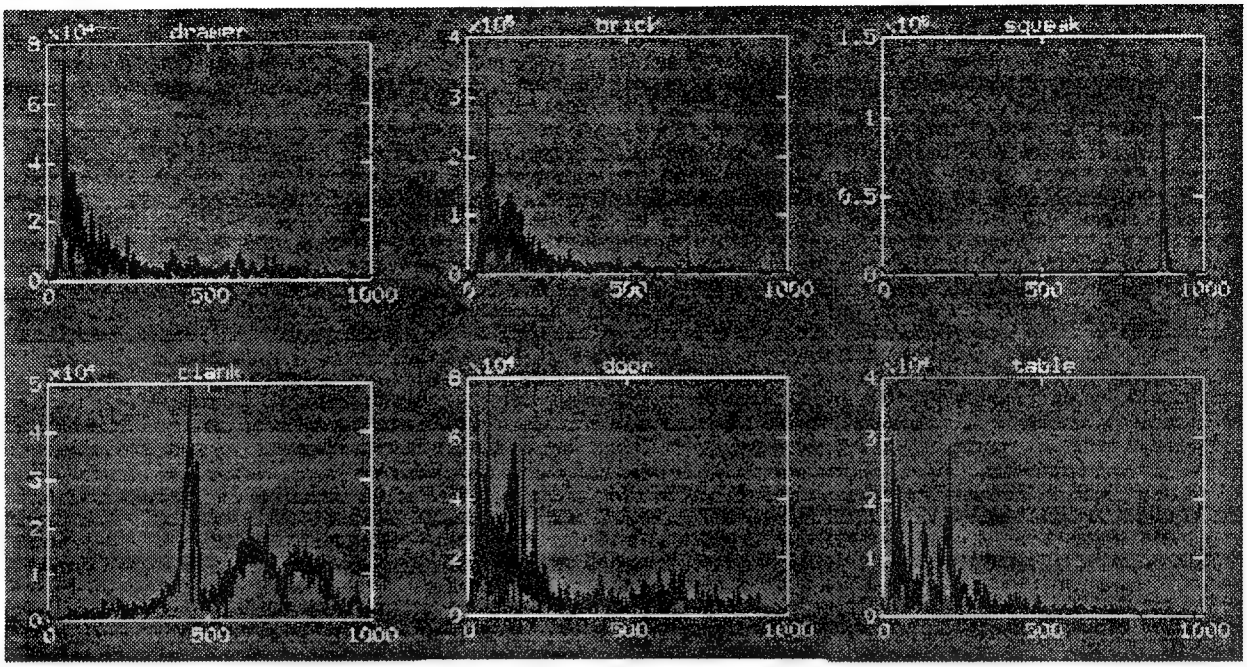

Figure 9. Fourier transform of one signal from each class.
Top row left to right: drawer, brick, squeak. Bottom row left to right: clank, door, table.

2.3. Navy Biologics Data Set

An introductory Navy biologics data set was acquired (originally from Woods Hole). This set consists of four classes of marine mammals. These signals were processed to segment out a subset of representative signals for classification tests. The signals obtained are listed in Table 2.

Source	Quantity
Sperm Whale Cries	195
Other Whale Cries	50
Porpoise	56
Dolphins	93
Shrimp Clicks	Numerous

Table 2. Biological Signals Extracted from Navy Data Tapes

Figure 10 shows the time-amplitude plot of one example from two classes: other whale cries and porpoise.

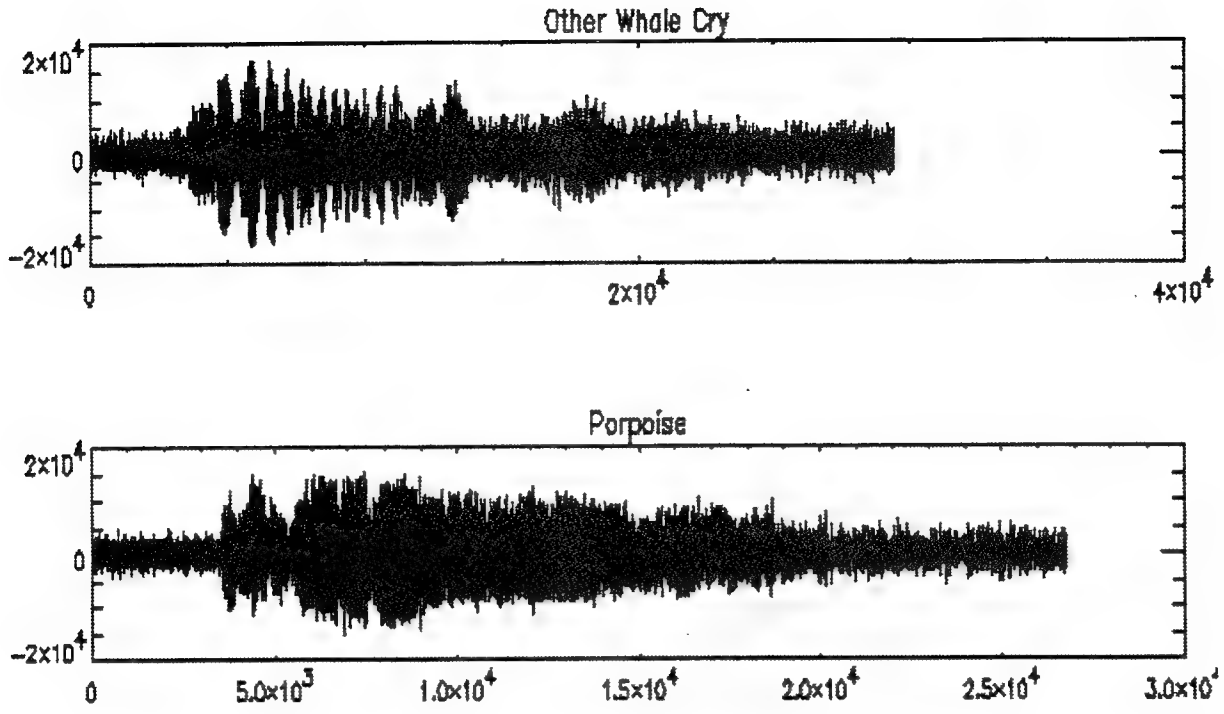

Figure 10. Time-amplitude history of two biological signals.

2.4. NUWC Classified Transient Databases

This NUWC Classified Transient Database consists of a wide variety of signals obtained from diverse sensors in different environments. It is a compilation of signals obtained from various recent Navy exercises. Conditions vary significantly. A variety of acoustic sensors are represented whose characteristics are extremely varied. These variations make it difficult to perform comparative testing using this database since the sensor characteristics often overshadow the signals. However, certain classes of significant signals were extracted with consistent sensor characteristics.

These classes included some cooperative exercises in which a wrench was repeatedly dropped. Other cooperative exercises included repeated dives to produce a database of hull pops associated with pressure effects. Individual pulses from a bilge pump were also extracted although one would generally classify pumps based on the pump frequency rather than the properties of each individual pulse. Several mast and periscope related transient events were extracted but not in sufficient numbers to train a classifier.

The variations in the database made it difficult to use much of it; however, the signal detection algorithm was validated using this data since some of the variations represent real world variations. However, a real system would only have a single sensor.

2.5. Synthetic Generic Transient Databases

Our original concept for exploiting transients for ASW was to detect and identify submarine unique transients. However, Navy documents and our analysis of the MSF's Sea Test Data have indicated the probability of occurrence of submarine unique transients is too low to be relied upon for MSF missions. Our data analysis has revealed that there are a very large number of transients produced by man-made vessels. These transients cannot be uniquely identified according to their source. However, they do fall into four general classes referred to as generic transients. The detection of an increase in generic transients is a strong indication that some object is passing near the sensors. In order to investigate the theory, we have created a synthetic database of generic transients based upon Navy documents in Navy Journal of Underwater Acoustics [1] and our own analysis.

Four classes of generic transient types were defined which include most of the observed underwater transients. They are Type I (impulse), Type II (ringing), Type III (chirp) and Type IV (noise-like) transients. Functionally the Type I and Type II are similar except that the decay is extremely rapid for Type I and there are harmonics in Type II. We have found that objects of interest produce a large number of Type I and II transients that cannot be identified by their source. Type IV is essentially band limited Gaussian noise often associated with air discharges. These synthetic transients were generated based on observations of real acoustic data according to the parameters in Table 3.

Signal Class	Center Frequency	Duration	Harmonics	Bandwidth	Detection Threshold
I) Impulse	2000-3000 Hz	5-10 ms	0	narrow	0.25
II) Ringing	600-1000 Hz	100-200 ms	2	narrow	0.25
III) Chirp	330-400 Hz	80-120 ms	2	narrow	0.25
IV) Noise-like	2000-3000 Hz	200-500 ms	0	1400-1800 Hz	0.5

Table 3. Generic Transient Signal Classes and Parameters

Figure 11 shows a representative signal for each generic transient type.

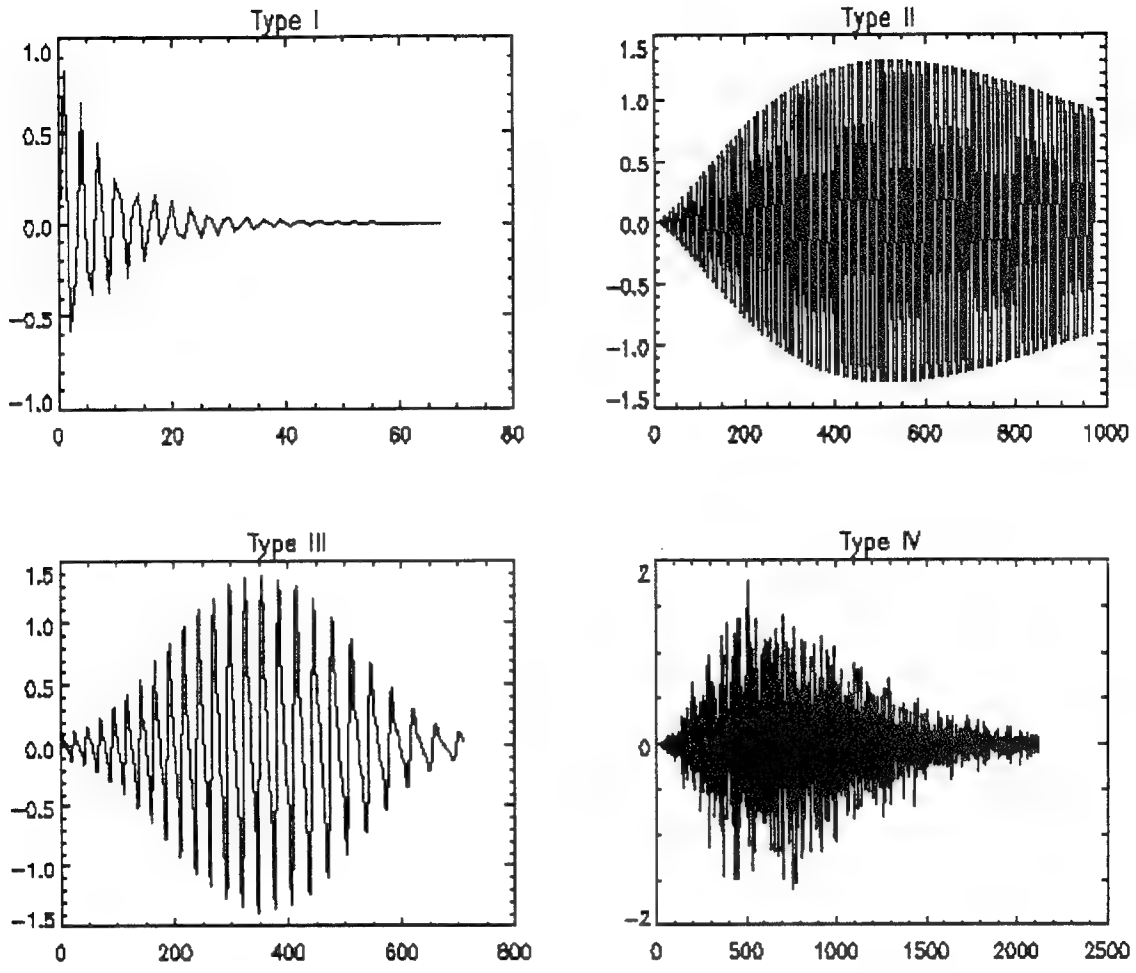

Figure 11. Generic Transient Signals

An extended generic transient data set has also been generated to permit within-class tests. For each of the four classes of generic transients, subclasses were generated using a model which best fits the shape of the given transient type. Subclasses are generated by varying the parameters of the model.

(I) The model used for the impulsive transients (Type I) was

$$y(t) = \sin(2\pi t F_c)\,\Gamma(\alpha, \beta)$$

The parameters used to generate the impulsive transient subclasses are given in Table 4.

Type I Signal Subclass	Center Frequency *Fc*	Duration	α	β
A	2500 Hz	5-6 and 8-10 ms	2.5	2.5
B	2000-2400 and 2600-3000 Hz	7 ms	2.5	2.5
C	2500 Hz	7 ms	1-2 and 3-4	2.5
D	2500 Hz	7 ms	2.5	0.5-2 and 3-4

Table 4. Impulsive Transient Signal Subclasses and Parameters

(II) The model used for the ringing transients (Type II) was

$$y(t) = s(t)\,\Gamma(\alpha, \beta)$$

where

$$s(t) = s_1(t) + s_2(t) + s_3(t)$$
$$s_1(t) = \sin(2\pi t F_c)$$
$$s_2(t) = 0.5\sin(2\pi t(F_c + F_c))$$
$$s_3(t) = 0.25\sin(2\pi t(F_c + F_c + F_c))$$

The parameters used to generate the ringing transient subclasses are given in Table 5.

Type II Signal Subclass	Center Frequency *Fc*	Duration	α	β
A	800 Hz	100-125 and 175-200 ms	2.5	2.5
B	600-700 and 900-1000 Hz	150 ms	2.5	2.5
C	800 Hz	150 ms	1-2 and 3-4	2.5
D	800 Hz	150 ms	2.5	0.5-2 and 3-4

Table 5. Ringing Transient Signal Subclasses and Parameters

(III) The model used for the chirp transients (Type III) was

$$y(t) = s(t)\,h(t)$$

where:

$$s(t) = s_1(t) + s_2(t) + s_3(t)$$
$$s_1(t) = \sin(2\pi t F(t))$$
$$s_2(t) = (\sin(2\pi t(F(t) + F(t))))/(mag)$$

$s_3(t) = (0.5 \sin(2\pi t(F(t) + F(t) + F(t))))/(mag)$
$F(t)$ = Frequency function which starts at F_c at time = 0 and ends at $(1 - slide)*F_c$ at time = t

The parameters used to generate the chirp transient subclasses are given in Table 6.

Type III Signal Subclass	Center Frequency *Fc*	Duration	slide	mag
A	365 Hz	80-90 and 110-120 ms	0.25	2
B	365 Hz	100 ms	.1-.2 and .3-.5	2
C	330-360 and 370-400 Hz	100 ms	0.25	2
D	365 Hz	100 ms	0.25	1.5-1.75 and 2.25-2.5

Table 6. Chirp Transient Signal Subclasses and Parameters

(IV) The model used for the noise-like transients (Type IV) was

$$y(t) = s(t)\,\Gamma(\alpha, 1)$$

where $s(t)$ = bandpass filtered noise (FIR type filter)

The parameters used to generate the noise-like transient subclasses are given in Table 7.

Type IV Signal Subclass	Center Frequency *Fc*	Duration	α	bandwidth
A	2500 Hz	200-300 and 400-500 ms	3	1600 Hz
B	2000-2400 and 2600-3000 Hz	350 ms	3	1600 Hz
C	2500 Hz	350 ms	3	1400-1500 and 1700-1800 Hz
D	2500 Hz	350 ms	1.5 -2.5 and 3.5-4.0	1600 Hz

Table 7. Noise-Like Transient Signal Subclasses and Parameters

3. TRANSFORMS

Two major types of transform were used in this study: the Wavelet and the Fourier transforms. Within the Wavelet family, we have implemented the Daubechies Discrete Wavelet Transform (DWT), the Gauss-Morlet Continuous Wavelet Transform (CWT), and the M-Band Wavelet Transform. For the Fourier family, we have implemented the Short-Time Fourier Transform (STFT), the Gabor Transform, the Wigner-Ville Distribution (WVD), and the Choi-Williams Distribution (CWD). These transforms are described below.

3.1. Continuous Wavelet Transform (Scalogram)

The Continuous Wavelet Transform [2, 3] can be expressed as an inner product of the form

$$CWT(t, a) = \int x(\tau)\, h_{a,t}^{*}(\tau)\, d\tau$$

which measures the "similarity" between the signal and the basis functions.

$$h_{a,t}(\tau) = \frac{1}{\sqrt{|a|}} h\left(\frac{\tau - t}{a}\right)$$

called wavelets. The wavelets are scaled and translated versions of the basic wavelet prototype $h(t)$.

A typical continuous wavelet is the Morlet wavelet which is a complex sinusoid windowed with a Gaussian envelope. The range for the scale a is {1.0, 2.0, 3.1, 3.2, 3.3, 3.4, 5.0, 6.0} with emphasis placed in the region around 3.1 to 3.4.

3.2. Discrete Wavelet Transform

A special case of the general family of wavelet transforms is when $a = a_0^n$ where $a_0 = 2$ and n is an integer.

$$DWT(t, n) = \frac{1}{\sqrt{a_0^n}} \int x(\tau)\, h\left(\frac{\tau - t}{a_0^n}\right) d\tau$$

In the discrete case, we can describe the Discrete Wavelet Transform as follows. The (single-stage) DWT operates on a sequence s to yield two sequences

$$s_1(k) = \sum_{n=0}^{N-1} \bar{h}(n)s(2k+n)$$

$$w_1(k) = \sum_{n=0}^{N-1} \bar{g}(n)s(2k+n)$$

where h is a wavelet-parameter sequence that satisfies conditions described by Daubechies and the sequence g is defined by $g(k) = (-1)^k \bar{h}(N-1-k)$ In particular, h and g form a pair of lowpass and highpass conjugate quadrature filter and the two corresponding sequences s_1 and w_1 constitute level-1 lowpass and highpass subbands. The L-level multistage DWT is obtained by recursive single-stage DWT of the lowpass subbands s_{L-1} to yield sequences $s_L, w_L, \ldots w_1$.

Examples of wavelet-parameter sequences include:

Haar: D2 = $\{\frac{\sqrt{2}}{2}, \frac{\sqrt{2}}{2}\}$

Daubechies-4: D4 =

$$\{\frac{1+\sqrt{3}}{4}, \frac{3+\sqrt{3}}{4}, \frac{3-\sqrt{3}}{4}, \frac{1-\sqrt{3}}{4}\}$$

The DWT is invertible since the special conditions on wavelet-parameters imply

$$s(k) = \sum_n h(k-2n)s_1(n) + \sum_n g(k-2n)w_1(n)$$

Therefore, the DWT preserves all information in the original sequence. Furthermore, each entry of the DWT is a linear functional of the original sequence that is localized in both position (since h has finite length) and in scale (a consequence of the relationship between the DWT and wavelet bases). If the sequence s represents a sampled signal of continuous time, then the subbands represent samples of a near octave-frequency subband decomposition of s.

3.3. M-Band Discrete Wavelet Transform

The M-Band Discrete Wavelet Transform [4] in general refers to the special case where $a = a_0^n$ with a_0 = M and n is an integer. Decomposition into M subbands is applied recursively to the low frequency.

3.4. Short-Time Fourier Transform (Spectrogram)

The standard Fourier analysis allows the decomposition of a signal into individual frequency components and establish the relative intensity of each component. The energy spectrum does not, however, explicitly show the time localization of the frequency components. But such a time

localization can be obtained by suitably pre-windowing the signal $x(t)$ as is done in the Short-Time Fourier Transform [5].

$$STFT(t, \omega) = \int x(\tau)\, g(\tau - t)\, e^{-j\omega\tau} d\tau$$

where $g(t)$ is a window function.

3.5. Gabor Transform

Gabor Transform is a special case of STFT where the window is a Gaussian window. Gaussian windows are often used since they meet the bound with equality for the Heisenberg inequality or uncertainty principle.

3.6. Pseudo-Wigner-Ville Distribution

The Wigner-Ville Distribution [6, 7] can be thought of as a time-varying power spectral density computed as the Fourier transform of a time-varying instantaneous estimate of an auto-correlation function. The original Wigner-Ville Distribution has high time-frequency concentration. The cross term oscillations of relatively high frequencies can be greatly reduced by using a low-pass filter at the expense of autocomponent broadening. The pseudo-Wigner-Ville Distribution is given by

$$PWVD(t, \omega) = \int x(t + \frac{\tau}{2})\, x^*(t - \frac{\tau}{2})\, h(\tau)\, e^{-j\omega\tau} d\tau$$

where $h(t)$ is a low-pass filter.

3.7. Choi and Williams Distribution

The Choi-Williams distribution preserves the signal energy marginals, and for some signals offers substantial cross-term suppression with little autocomponent broadening.

$$CWD(t, \omega) = \iint \sqrt{\frac{\sigma}{4\pi\tau^2}}\, exp\left(-\frac{\sigma(\mu - t)^2}{4\tau^2}\right) x(\mu + \frac{\tau}{2})\, x^*(\mu - \frac{\tau}{2})\, e^{-j\omega\tau} d\mu d\tau$$

4. DETECTION

Transient signals can be detected either in the time domain or in a transform domain. Under wideband ambient noise conditions detection of a transient in the time domain may be inefficient especially if the transient signal has significant components on discrete elements of the transform

space, i. e. frequency, signal shape [8]. Consequently, we have concentrated our approach to detection using STFT and DWT. A version of the Wolcin sequential detector was used which produces a statistic consisting of the maximum likelihood signal power estimates in frequency and time. The Wolcin detector also adaptively estimates and updates the noise power spectral density.

4.1. Generalized Likelihood Ratio (GLR) Detector

Consider the following detection problem:

$$H_0: x(t) = n(t)$$

$$H_1: x(t) = s(t) + n(t)$$

where $x(t)$ is the received signal, $s(t)$ is the transient which is a time-localized signal waveform, $n(t)$ is a Gaussian noise of spectral density $\sim N(0, 1)$

It can be shown that the above detection problem is equivalent to

$$H_0: x = n$$

$$H_1: x = s + n$$

where x, s, and n are the Fourier Transform or Wavelet Transform coefficients of $x(t)$, $s(t)$, and $n(t)$ respectively.

We now derive a detector based on the following generalized likelihood ratio (GLR) testing statistic:

$$\Lambda_{GLRT}(x) = \frac{p(x|_{H_1})}{p(x|_{H_0})}$$

where $x|_{H_0} \sim N(\mu_0, \sigma_0^2)$ and $x|_{H_1} \sim N(\mu_1, \sigma_1^2)$

The testing statistic is compared against a threshold ς to determine if a signal is present:

$$\text{Accept } H_0 \text{ if } \quad \frac{(x-\mu_0)^2}{\sigma_0^2} - \frac{(x-\mu_1)^2}{\sigma_1^2} < \varsigma$$

$$\text{Accept } H_1 \text{ if } \quad \frac{(x-\mu_0)^2}{\sigma_0^2} - \frac{(x-\mu_1)^2}{\sigma_1^2} > \varsigma$$

More specifically, let $d_1(\xi), d_2(\xi)$ be the roots to the quadratic equation

$$ap(x)^2 - bp(x) + c = 0$$

where $a = \sigma_1^2 - \sigma_0^2$, $b = -2(\mu_0\sigma_1^2 - \mu_1\sigma^2{}_0)$, and $c = \mu_0^2\sigma_1^2 - \mu_1^2\sigma_0^2 - \xi$

Then $d_1(\xi), d_2(\xi)$ are given by

$$\frac{(\mu_0\sigma_1^2 - \mu_1\sigma_0^2) \pm \sqrt{(\mu_0\sigma_1^2 - \mu_1\sigma_0^2)^2 + (\sigma_1^2 - \sigma_0^2)(\mu_0^2\sigma_1^2 - \mu_1^2\sigma_0^2 - \xi)}}{\sigma_1^2 - \sigma_0^2}$$

The decision boundary for the Generalized Likelihood Ratio Detector can now be expressed as

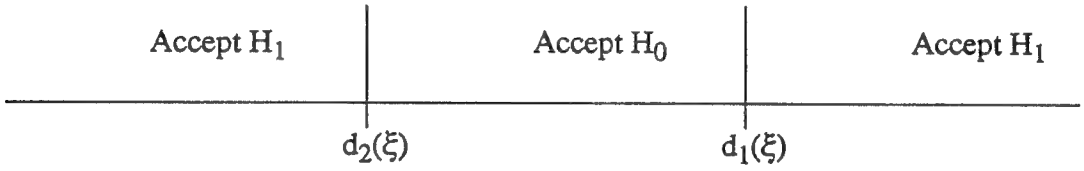

The probability of detection (PD) and probability of false alarm (PFA) can now be analytically expressed as

$$PD = \Phi\left(\frac{d_2(\xi) - \mu_1}{\sigma_1}\right) + 1 - \Phi\left(\frac{d_1(\xi) - \mu_1}{\sigma_1}\right)$$

$$PFA = \Phi\left(\frac{d_2(\xi) - \mu_0}{\sigma_0}\right) + 1 - \Phi\left(\frac{d_1(\xi) - \mu_0}{\sigma_0}\right)$$

where Φ is the error function defined by $\Phi(t) = \frac{1}{\sqrt{2\pi}} \int_{-\infty}^{t} e^{-\frac{x^2}{2}} dx$

4.2. Wolcin Detector Framework

Let $y(t)$ be a time series divided into K windows where each window is of length L. The input signal at each window is a vector of L elements. The transform of the input vector is an output vector of L' elements. At this point, we assume that successive windows do not overlap although

our approach does not preclude this. Let $\tilde{Y}_{kl}$ ($k = 1, 2, ..., K$ and $l = 1, 2, ..., L'$) be the value of the l^{th} bin in the transform of the k^{th} window on $y(t)$. The bins can be either the frequency bins in the case of Fourier Transform or the scale bins for Wavelet Transform.

The WolcinWolcin detector adaptively estimates and updates the noise power spectral density as described below. The background noise power spectral density is initialized by estimating an average over a set of K' windows.

$$\tilde{Z}_{K',l} = \frac{1}{K'} \sum_{k=1}^{K'} \tilde{Y}_{k,l}$$

At $k = K' + 1$, $Z_{k-1,l} = \tilde{Z}_{K',l}$. After the background noise vector $Z_{k-1,l}$ is established at the k^{th} ($k > K'$) window, one can normalize the subsequent windows of transform as

$$Y_{k,l} = \tilde{Y}_{k,l} / Z_{k-1,l}$$

The noise power spectral estimates are adaptively updated as follows:

$$Z_{k,l} = (1-\alpha) Z_{k-1,l} + \alpha \tilde{Y}_{k,l} \qquad \text{for } Y_{k,l} \geq 1 + S_0$$

and $$Z_{k,l} = Z_{k-1,l} \qquad \text{for } Y_{k,l} < 1 + S_0$$

Here S_0 is the hard threshold to determine whether a signal may be present at the l^{th} bin. The parameter 'α' is the 'forgetting factor'. The effect of α is to make the background noise vector adapt to the slow and subtle changes of the environment such as temperature gradient or light intensity. The value of S_0 is dependent on the requirement or acceptable performance. One can choose a small value of S_0 to increase the PD or a large value of S_0 to reduce the PFA.

4.3. STFT Based Generalized Likelihood Ratio Detector

As described in Section 4.1, the detection problem can be formulated in terms of the Fourier coefficients of the received signals. The detector in this case is given by

$$d(Y) = \sum_k \sum_l X_{k,l} \qquad \text{where}$$

$$X_{k,l} = Y_{k,l} - 1 - ln(Y_{k,l}) \qquad \text{for } Y_{k,l} \geq 1 + S_0$$

$$X_{k,l} = 0 \qquad \text{for } Y_{k,l} < 1 + S_0$$

Let $N = KL/2$ be the total number of time-frequency bins considered. (Recall K is the total number of windows, L is the length of the window). If N is sufficiently large then we can use the Central Limit Theorem to approximate $d(Y)$ as a Gaussian random variable:

$d(Y)\big|_{H_0} \sim N(\mu_0, \sigma_0^2)$: and $d(Y)\big|_{H_1} \sim N(\mu_1, \sigma_1^2)$ where the parameters are given below.

Hypothesis H_0: Noise only

$$\mu_0 = N\mu \quad \text{where} \quad \mu = \int_{1+S_0}^{\infty} (x - 1 - ln(x))\, e^{-x} dx$$

$$\sigma_0 = N\sigma \quad \text{where} \quad \sigma^2 = \left[\int_{1+S_0}^{\infty} (x - 1 - ln(x))^2 e^{-x} dx - \mu^2 \right]^{1/2}$$

Hypothesis H_1: Signal and Noise

$$\mu(S_0, S_p) = \int_{1+S_0}^{\infty} \frac{1}{1+S_p} (x - 1 - ln(x))\, e^{-\frac{x}{1+S_p}} dx$$

$$\mu_1 = (N-P)\,\mu + \sum_{p=1}^{P} \mu(S_0, S_p)$$

$$\sigma(S_0, S_p) = \left[\int_{1+S_0}^{\infty} \frac{1}{1+S_p} (x - 1 - ln(x))^2 e^{-\frac{x}{1+S_p}} dx - \mu(S_0, S_p)^2 \right]^{1/2}$$

$$\sigma_1 = (N-P)\,\sigma + \sum_{p=1}^{P} \sigma(S_0, S_p)$$

Here it is assumed the signal is present in P out of N Time-Frequency bins. S_p is the signal mean power on the p^{th} bin.

4.4. Wavelet Based Generalized Likelihood Ratio Detector

Concatenate the time series $Y_{k,l}$ into a vector $\hat{y}$ with L elements and use a sampled wavelet function W at various scales and time shifts to represent $\hat{y} = W\hat{a} + \hat{v}$ where

$$W = \begin{bmatrix} w_{11}(t_1) & \cdots & w_{11}(t_L) \\ \cdots & \cdots & \cdots \\ \cdots & w_{nm}(t_l) & \cdots \\ \cdots & \cdots & \cdots \\ w_{NM}(t_1) & \cdots & w_{NM}(t_L) \end{bmatrix}$$

w_{nm} is the basic wavelet at scale n and time-shift index m. In the above representation, the time series is expressed as linear combination of scaled and shifted versions of a wavelet. $\hat{v}$ is additive gaussian noise.

Apply a wavelet transform to $\hat{y}$ by multiplying it with another wavelet matrix $\boldsymbol{R}$. $\boldsymbol{R}$ does not have to be the same as $\boldsymbol{W}$ and it can incorporate a priori knowledge about the nature of transient signal we are trying to detect. Also the dimensions of $\boldsymbol{W}$ and $\boldsymbol{R}$ can be different The rows of $\boldsymbol{R}$ need not be orthogonal. The transformation results in: $\boldsymbol{R}\hat{y} = \boldsymbol{RW}\hat{a} + \boldsymbol{R}\hat{v}$

The generalized likelihood ration (GLR) testing statistic in this case is

$$x = \hat{y}\boldsymbol{R}^c\boldsymbol{R}\boldsymbol{W}(\boldsymbol{W}^c\boldsymbol{R}^c\boldsymbol{R}\boldsymbol{W})^{-1}\boldsymbol{W}^c\boldsymbol{R}^c\boldsymbol{R}\hat{y}$$

or Accept H_0 if $(x = \hat{y}\boldsymbol{P}_{\boldsymbol{W}|\boldsymbol{R}}\hat{y}) \leq \eta$

Accept H_1 if $(x = \hat{y}\boldsymbol{P}_{\boldsymbol{W}|\boldsymbol{R}}\hat{y}) \geq \eta$

where $$\boldsymbol{P}_{\boldsymbol{W}|\boldsymbol{R}} = \boldsymbol{R}^c\boldsymbol{R}\boldsymbol{W}(\boldsymbol{W}^c\boldsymbol{R}^c\boldsymbol{R}\boldsymbol{W})^{-1}\boldsymbol{W}^c\boldsymbol{R}^c\boldsymbol{R}$$

x is statistically distributed as a χ^2 random variable.

Under the H_0 hypothesis x is a central χ^2 with $2NM$ degrees of freedom when the data are complex-valued and of NM degrees of freedom when they are real-valued. The probability density function of x under H_0, assuming $2NM$ degrees of freedom, is given by

$$p_0(x) = \frac{1}{\sigma^{2NM}2^{NM}\Gamma(NM)}x^{NM-1}exp\left(\frac{-x}{2\sigma^2}\right)$$

Under H_1, the probability density function for x is:

$$p_1(x) = \frac{1}{2\sigma^2}\left(\frac{x}{S}\right)^{\frac{NM-1}{2}} exp\left(\frac{-(x+S)}{2\sigma^2}\right) I_{NM-1} exp\left(\frac{\sqrt{Sx}}{\sigma^2}\right)$$

where I_{NM-1} is the zeroth order Bessel function and $\Gamma()$ is the gamma function and S is the signal power given by: $S = \sum_{i=1}^{NM} |s_i|^2$ where s_i is the signal component from the projection of the signal on the i^{th} column of $P_{W|R}$.

5. FEATURE EXTRACTION

The Wavelets program has the goal of performing comparative tests of wavelets based approaches to a variety of classical time-frequency transform based techniques for signal detection and identification. A prerequisite for this comparison is the generation of robust shift invariant features for each of the techniques included in the comparative tests. The large dimensionality of observation vectors, consisting of digital samples of an interval of received acoustic signal, precludes using observation vectors as feature vectors because impractically large training sets and excessive computation would be required. Reduction of dimensionality, achieved by mapping observation vectors to smaller dimensional feature vectors, is required. Time-frequency (STFT, Wigner-Ville), time-scale (Wavelet), and related Conjugate Quadrature Filter [9] transforms promise to provide low-dimensional, and therefore computationally tractable, feature vectors whose class densities are sufficiently distinct to classify transients.

Two related problems consist of (1) selecting optimal transforms (or combinations thereof) and (2) defining optimal features as functions of the transformed signal. Each class density of the feature vector should be compact, invariant with respect to translation of the observation vector, and separated from other class densities. For instance, wavelet coefficients exhibit strong dependence on the signal phase. However, energy/temporal-spread features based on computing the sum of and the spread of squared wavelet coefficients within each band are nearly translational invariant. Our studies using various transforms, including Wave Packets, M-band, and hierarchical versions of the Daubechies wavelet, indicated they also provide nearly translational invariant features that effectively separate transient classes.

Feature extraction is performed following transient detection and segmentation. Since segmentation in the presence of noise is an error prone operation, one can expect differences in the signal start and end positions of a detected transient from event to event. Ideally feature extraction should show less variation due to sampling variation than to intraclass signal variation. Moment features were selected on the expectation that they would be shift invariant. They can be calculated for the original signal as well as for each decomposed band. The relative energy of each band to the total signal energy of the original signal should also be shift invariant.

5.1. Shift Invariant Band Moment Features

For typical classes of transient type signals, including classes of acoustic types, the gross signal energy distribution in position and scale (constant-Q frequency) is similar within the class and distinct between classes, whereas the point-to-point energies and the phase may vary as much within a class as between classes. These facts suggest that low-order moments of the squared moduli of a small number of wavelet subbands may provide low dimensional feature vectors for classifying transient signals [10]. Wavelet-band feature vectors for a signal are obtained by concatenating moments of each subband of a multistage DWT of the signal.

Moment based features are also extracted for the short-time Fourier transform. The moments of each transform frequency bin are calculated. The STFT was calculated with the same number of frequency bins as the number of scales used in the CWT transform.

In order to remove differences because of variation due to the signal amplitude and to mimic a probability density function the signal was normalized

$$w(t) = \frac{s^2(t)}{\int s^2(t)\,dt}$$

The d-th moment of band w_p is defined by

$$m_d(w_p) = \sum_k |w_p(k)|\ k^d$$

where $w_p(k)$ is defined in Section 3.2.

Since typical classes of signals may contain significant variation in the positions of the transients it is necessary to translate the transients $s(k)$ to a standard position prior to computing the DWT in order to obtain shift invariant wavelet-band feature vectors. This is accomplished by calculating the central moments.

The set of moment features used for classification were the statistical functions of the moments: the mean m_1, the standard deviation $(m_2)^{1/2}$, the skewness α_3 and kurtosis α_4.

$$\alpha_3 = \frac{m_3}{(m_2)^{3/2}}$$

$$\alpha_4 = \frac{m_4}{(m_2)^2}$$

5.2. Adaptive Energy Window Features

The most obvious feature in a Fourier time frequency spectrograms are peaks associated with each of the characteristic frequencies in the signal. Automatic techniques for exploiting spectral features for signal classification have been developed. Potentially the most accurate technique would locate the significant peaks and measure their widths and the energy associated with the peak. Automatic peak extraction can be difficult if the peak is broad or several peaks occur within a narrow frequency band.

The energy in local fixed size time-frequency regions can also be extracted with some loss in generality. Two techniques can be used for fixed size time-frequency regions, One uses a priori knowledge to pick the location of regions in the time-frequency domain. This works well if one has a physical model of the signal sources expected or if one is restricted to a limited variety of signals.

A more general approach uses adaptive region locations. Adaptive techniques place the fixed size regions on the maximum energy areas in the time-frequency domain. Simple algorithms avoid overlapping regions. For adaptive regions one obtains the energy in the region as well as the relative time and frequency location of the window as features for classification. Both the fixed and adaptive location techniques were exploited with time-frequency transforms on this program.

Wavelet transforms also exhibit peaks. Although wavelet transforms lack shift invariance, the overall shape of the transform changes slowly with time shifts. This should be expected since energy is conserved under a linear wavelet transform. Thus one can also extract shift invariant features based on the energy and location of adaptive regions. This technique was used for both discrete and continuous wavelet transforms.

Figure 12 compares the adaptive energy windows extracted for two examples in two different transient signal classes for the Daubechies discrete wavelet transform. (The horizontal time axes are at different scales depending on the segmentation process. One should compare the relative location of the windows for each class.) The trained classifier selected the energy content and scale of the first two windows as useful features but rejected the relative time.

6. CLASSIFICATION

Given a feature vector v, the maximum likelihood classifier [11, 12, 13]assigns the n-th class to v so as to maximize the likelihood $L(n|v) = P_n(v)P(n)$ where $P(n)$ is the a priori probability that the signal belongs to the n-th class, $P_n(v)$ is the class probability density, and $n = 1, \ldots, N$ with N = number of classes. The class probability densities can ben estimated either by a parametric density estimation procedure or a nonparametric density estimation procedure, such as Parzen or k-nearest neighbors. The high complexity of acoustic transient signals precludes the parametric density estimation procedures. The results presented here were generated using an implementation of Parzen windows known as Probabilistic Neural Networks (PNN) [14]. An enhanced PNN [15] that includes clustering and adoption of the Parzen kernel was also used. The adaptive PNN selects and uses the best features.

An alternative classifier known as Classification And Regression Tree (CART) [16] was also used. It employs linear combinations of features and also ranks the features in terms of discrimination

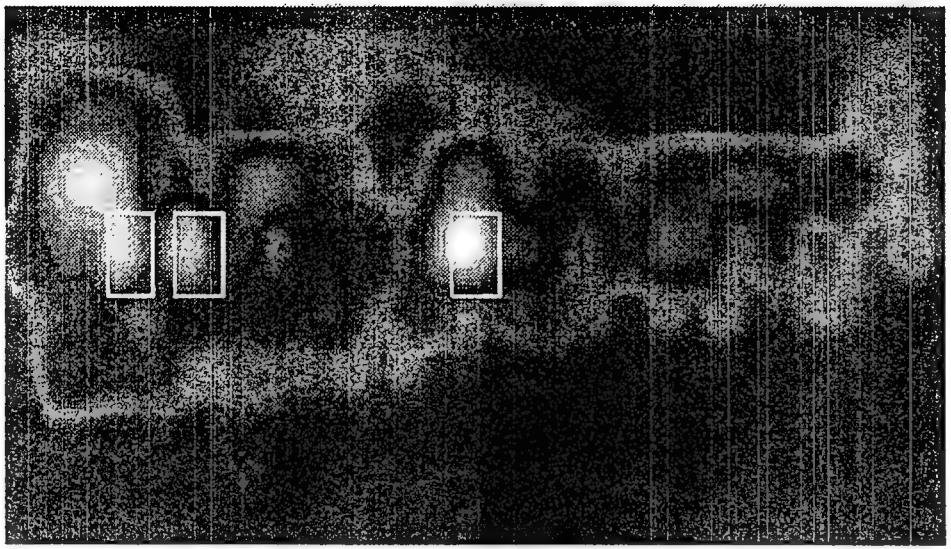

TABLE 1

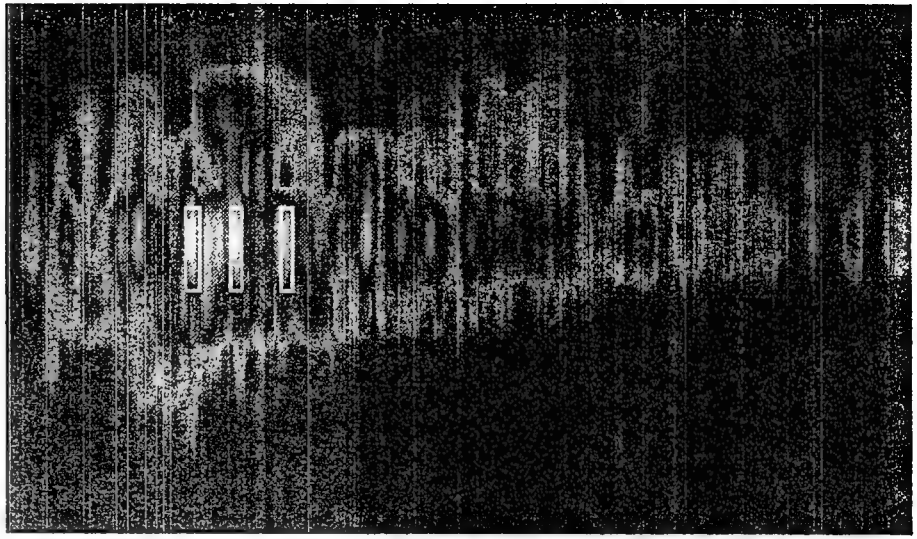

DRAWER 1

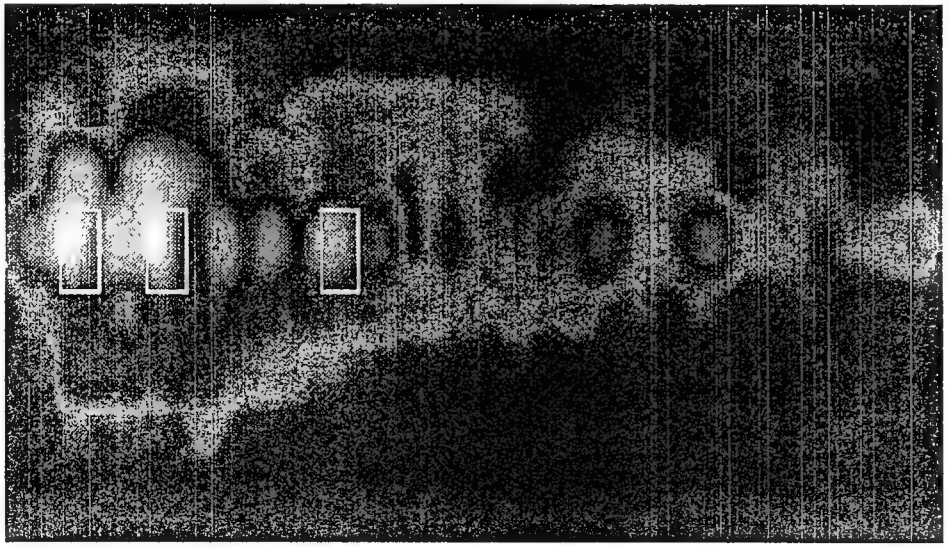

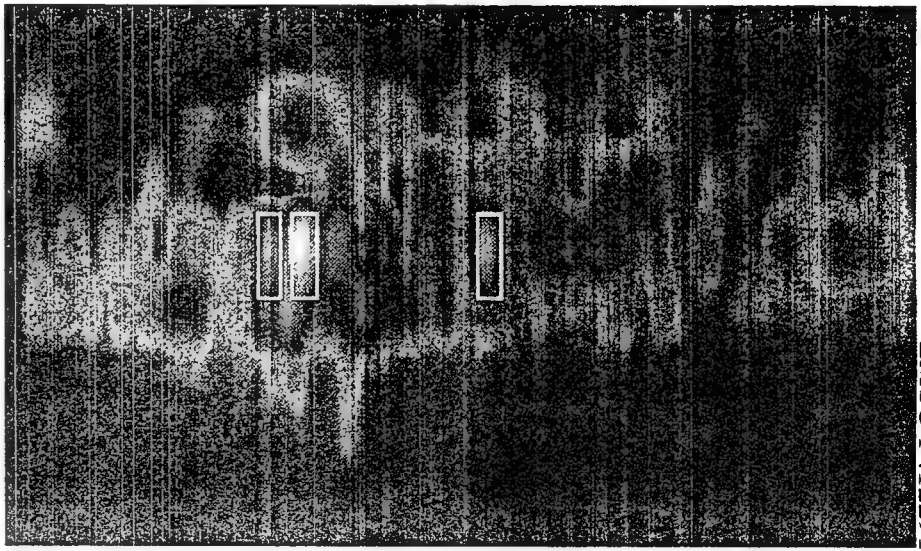

Figure 12. Top energy regions for the DWT of two table and two drawer transients.

power.

7. COMPARATIVE TESTS

7.1. Detection Comparative Tests

We have completed the development and implementation of both the STFT based generalized likelihood ratio detector and the DWT based generalized likelihood ratio detector. Both detectors use Wolcin weighting of noise background. The STFT detector has been transferred to the MSF Program where it is being used to analyze Sea Test data. Theoretical performance of both detectors, in terms of probability of detection (PD) versus probability of false alarm (PFA) curves, has been derived in close form as described in Section 4. Matlab and C codes of the performance measures have been written for both detectors.

We have completed a comparative tests between the two detectors using synthetic signals. To compare the performance of the detectors, both wideband and narrowband synthetic signals were generated and Monte Carlo tests conducted where 10,000 detections were performed using input signals with varying arrival time and noise. The PD versus PFA curves clearly indicated that the DWT detector does better than the STFT detector when the transients are wideband. When the signal is narrowband, however, STFT performs better than DWT. Here the signal is a single sinusoid.

We have also completed a comparative tests between the two detectors using generic signals. For each of the four generic transient types, a set of 10,000 noise-added transients with varying arrival time was generated to facilitate the detection comparative tests. More specifically, Gaussian noises with differing sigma were generated and added to the pure generic transients which have varying arrival time. The top figure of Figure 13 shows a representative impulsive transient (Type I) signal with a certain arrival time and the bottom figure shows the same transient with noise added to it. By viewing the bottom figure, one can not visually detect the arrival time of the transient. Figures 14-16 show the pure and noise-added transients for ringing, chirp and noise-like transients (Types II, III, and IV) respectively. Again, the arrival time in each case is not visually detectable in the time domain.

Both the STFT and the DWT detectors were applied to the four data sets. For each type and for each detector, the probabilities of detection (PD) and the probabilities of false alarm (PFA) were computed from the 10,000 detections. The PD versus PFA curves were plotted for each type and each detector and the curves are given in Figures 17 to 20. As can be seen in these figures, the STFT detector consistently performs much better than the DWT detector for all four generic types. For ringing (Type II) and chirp transients (Type III) in particular, the STFT detector is nearly perfect in detecting the arrival time of the transient with its PDs extremely close to 1 and its PFAs extremely close to 0.

7.2. Identification Comparative Tests

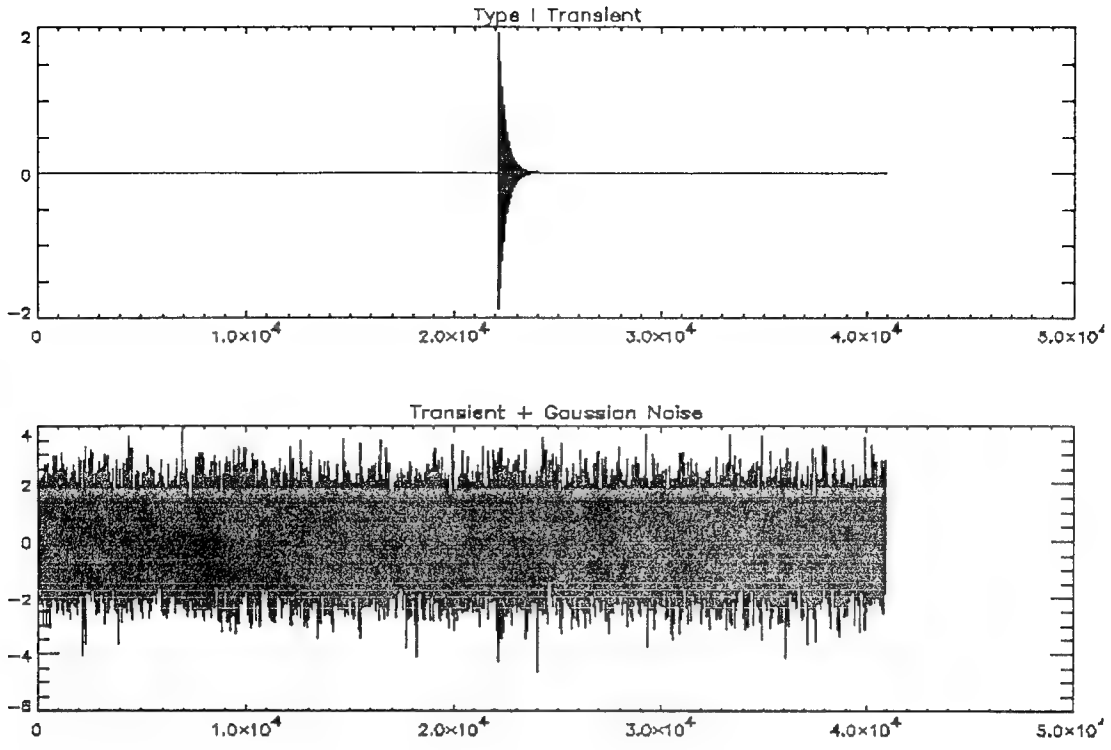

Figure 13. An impulsive transient signal (top) with noise added to it (bottom)

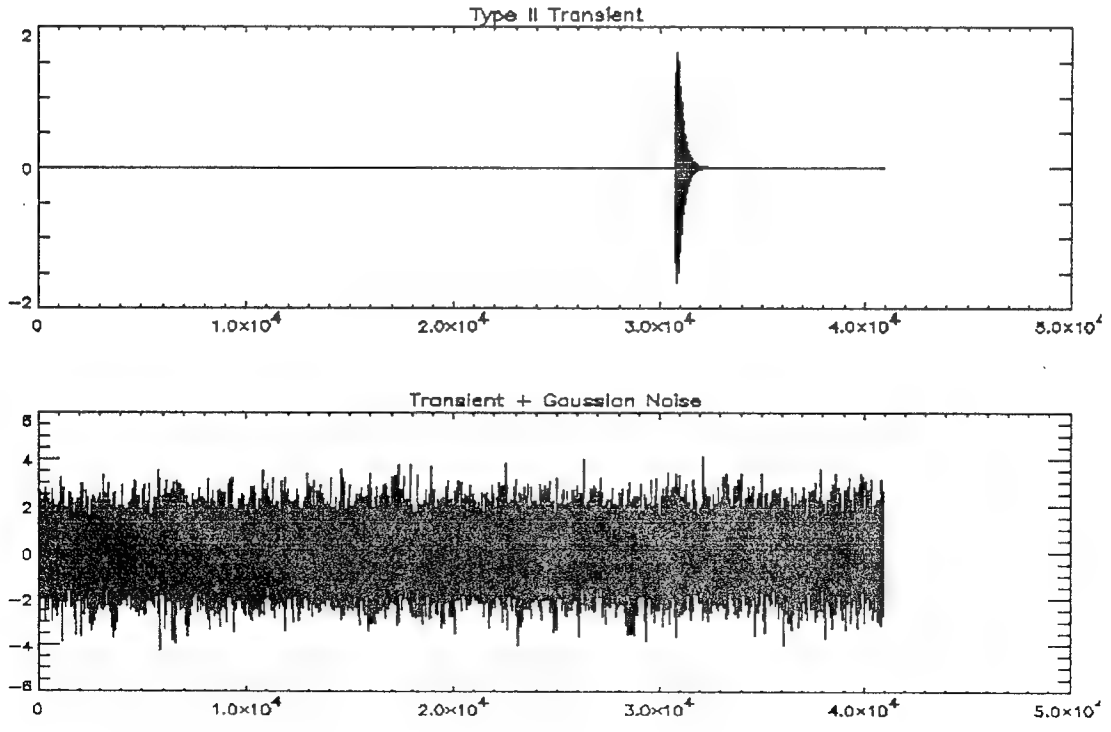

Figure 14. A ringing transient signal (top) with noise added to it (bottom)

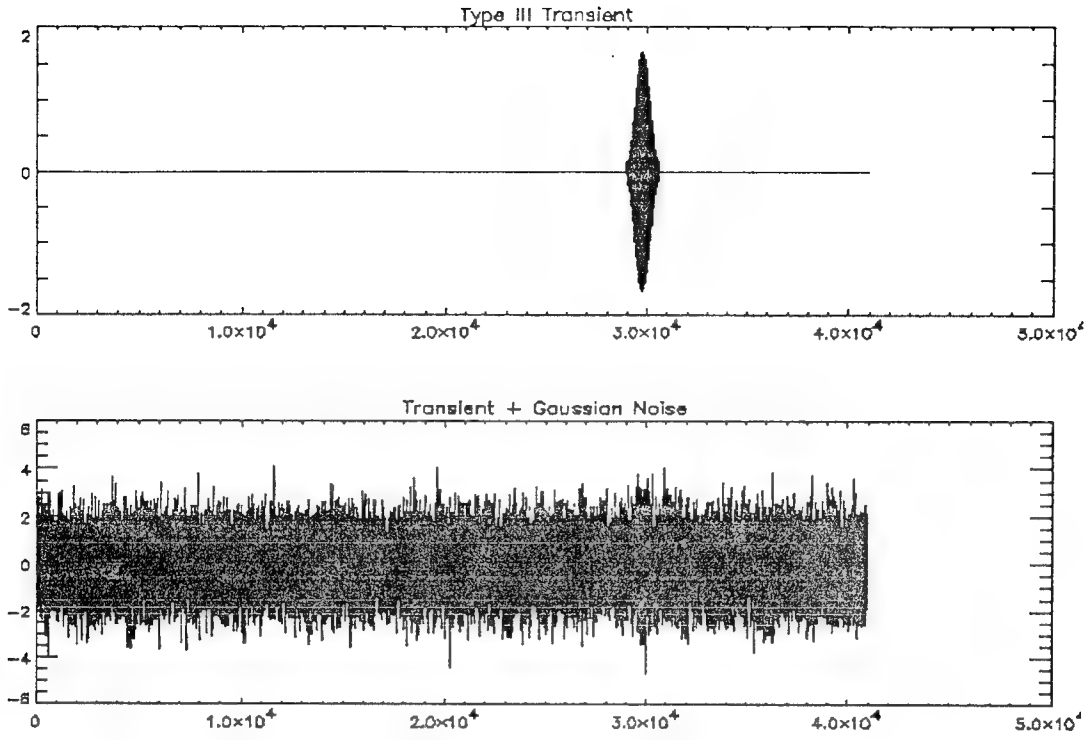

Figure 15. A chirp transient signal (top) with noise added to it (bottom)

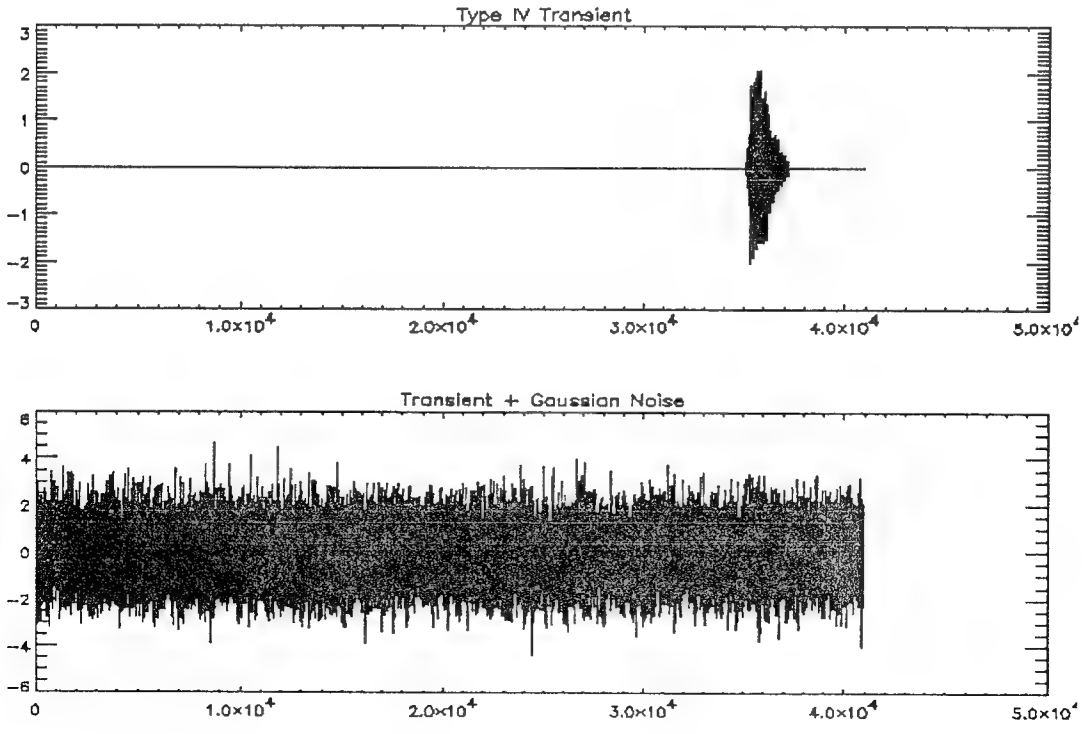

Figure 16. A noise-like transient signal (top) with noise added to it (bottom)

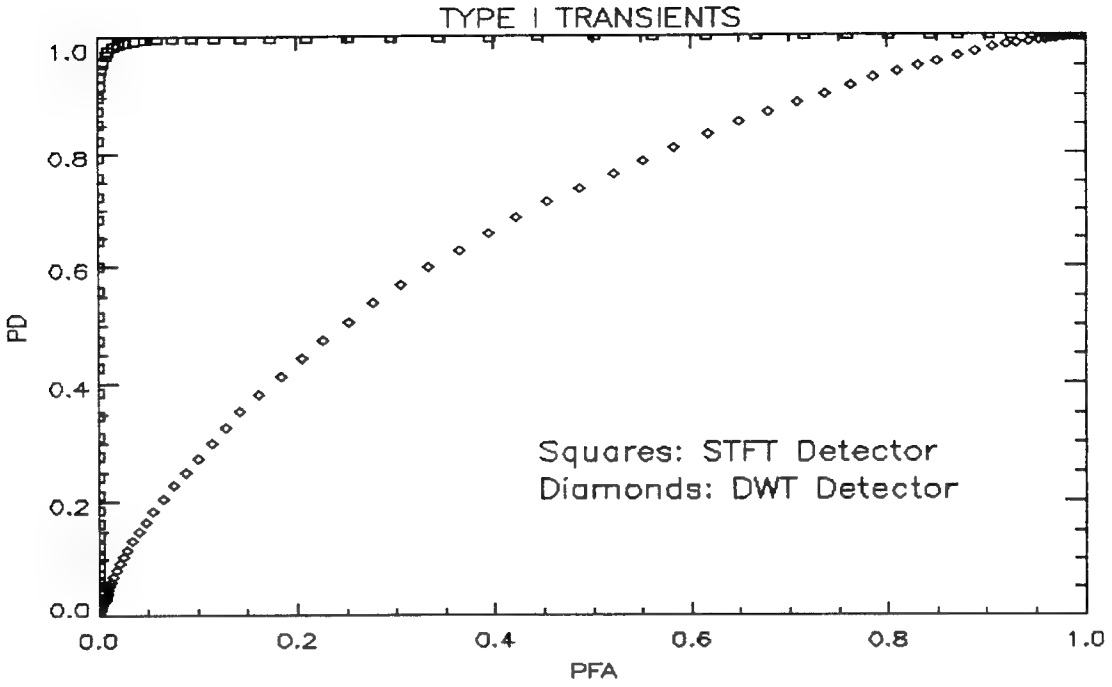

Figure 17. The PD vs. PFA curves for STFT and DWT detectors
Type I: Impulsive Transients

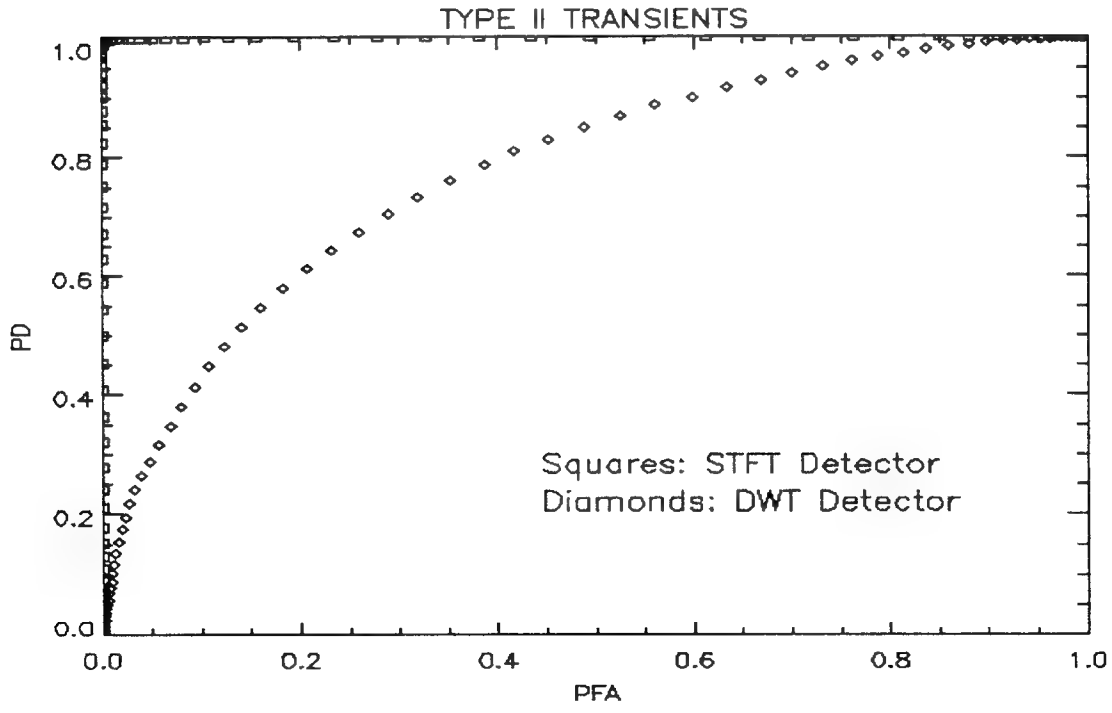

Figure 18. The PD vs. PFA curves for STFT and DWT detectors
Type II: Ringing Transients

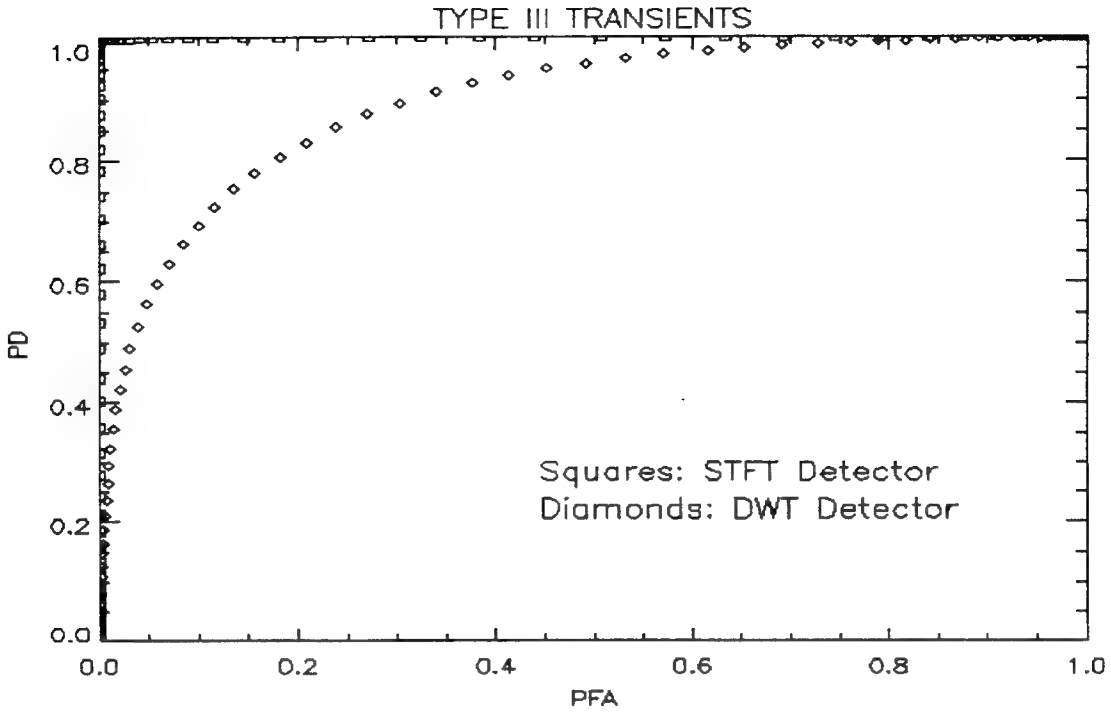

Figure 19. The PD vs. PFA curves for STFT and DWT detectors
Type III: Chirp Transients

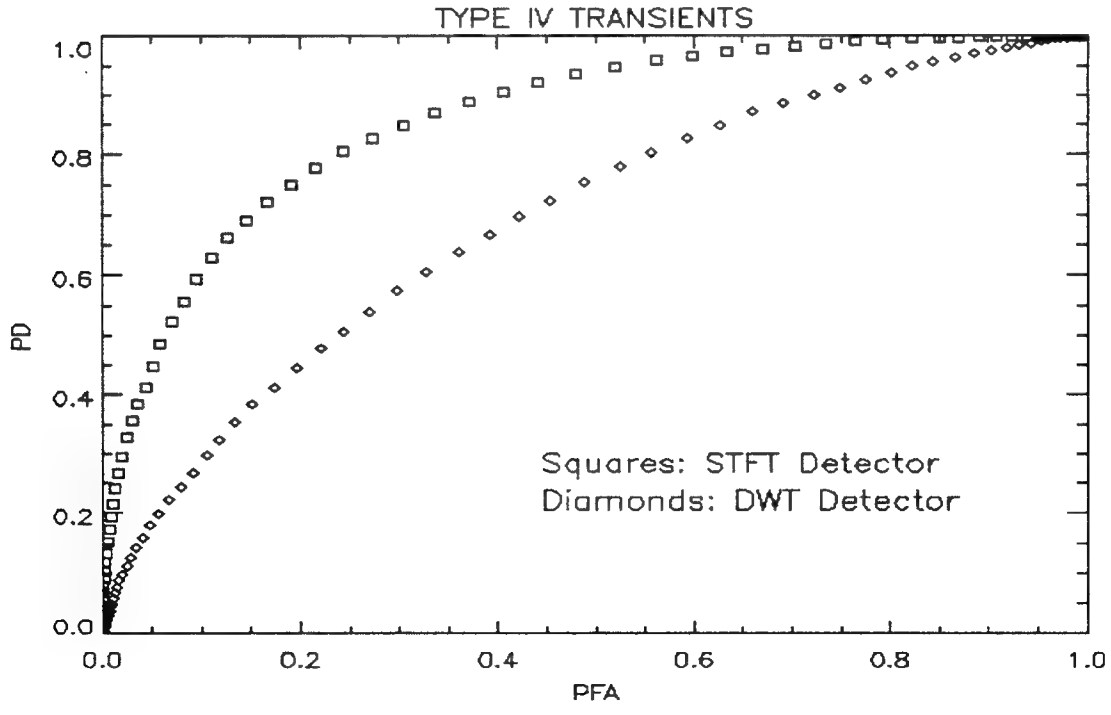

Figure 20. The PD vs. PFA curves for STFT and DWT detectors
Type IV: Noise-like Transients

Identification comparative tests were performed using the different combinations of features and transforms shown in Table 8.

Transform	Features
Discrete Wavelet Transform	Moments Adaptive Energy Windows
Continuous Wavelet Transform	Adaptive Energy Windows
Short Time Fourier Transform	Adaptive Energy Windows
Wigner-Ville Distribution	Adaptive Energy Windows
Constrained Total Least Squares	Frequency, Amplitude & Decay Coefficient for Poles

Table 8. Transforms and Features Used in Comparative Tests

7.2.1. Analysis of Homebrew Transient Test Set

We have completed the identification comparative test using the various candidate features and transforms on our homebrew transient set generated in the office. There were six classes of transients with 36 examples in each class. Classifier training was performed using 24 samples from each class and testing was performed on the remaining 12 samples. Table 9 shows the confusion matrix from CART using the DWT band moments. The confusion matrix is useful in

	DRAWER	BRICK	CLANK	DOOR	SQUEAK	TABLE
DRAWER	12	2	0	2	1	0
BRICK	0	8	0	0	1	1
CLANK	0	1	12	0	0	0
DOOR	0	0	0	10	0	0
SQUEAK	0	0	0	0	10	0
TABLE	0	1	0	0	0	11

Table 9. Confusion matrix for DWT wavelet moment band features.

examining false classifications. If the main error is between two related classes (i.e., brick and table are both excitations of the same system) then one is less concerned than if one has the same amount of error between unrelated classes. The misclassification of the nearly pure tone squeak with the broadband drawer and table is of concern [17].

Classification results based on wavelet band moment features were slightly better than adaptive energy window features derived using the STFT. These STFT features were obtained by

calculating the energy within three fixed size windows in time-frequency space. The STFT features used were the energy within each window and the location (relative time, frequency) of the center of the window. The classification results are shown in Table 10.

	DWT MOMENTS	CWT ENERGY	STFT ENERGY	WVD ENERGY
PNN	88	67	74	67
ADAPTIVE PNN	92		93	
CART	92	60	85	64

Table 10. Percent correct classification results.

The classification results for the continuous wavelet transform indicated that adaptive energy windows in time-scale space do not provide effective features. Additional research will be performed on feature selection using the continuous wavelet transform. Similarly the Wigner-Ville distribution performed poorly using adaptive energy windows. The choice of window size for both of these transforms should be examined since one would expect at least comparable performance to the STFT and discrete wavelet transform.

Relative feature rankings from CART (Table 11) and the adaptive PNN classifier indicate that the lower moments (mean and variance) of the subbands were more powerful discriminants than the higher order moments (skewness and kurtosis). The poorer performance of the high order moments is typical since they are more sensitive to noise processes.

RANKING	RELATIVE IMPORTANCE	SUBBAND	FEATURE
1	100	3	$(m_2)^{1/2}$
2	99	4	$(m_2)^{1/2}$
3	95	1	m_1
4	89	2	m_1
5	88	3	m_1
6	76	2	$(m_2)^{1/2}$
7	71	4	m_1
8	68	2	a_4
9	62	3	a_4
10	57	1	$(m_2)^{1/2}$
11	56	2	a_3

Table 11. Ranking of band moment features by CART

12	55	3	a_3
13	54	1	a_3
14	45	1	a_4
15	42	4	a_3
16	41	4	a_4

Table 11. Ranking of band moment features by CART

7.2.2. Analysis of Navy Biologics Data Set

An introductory Navy biologics data set was acquired (originally from Woods Hole). These signals were processed to extract features and classification results were obtained. Moment features extracted from the discrete wavelet transform were used to obtain a 75% correct classification rate using the first four classes in Table 2. Twenty examples of each class were reserved for testing and the rest were used for training. The confusion matrix is shown in Table 12. Misclassification of the porpoise and dolphins as whales seems to be the main error source. These signals have a considerable noise background.

	Sperm Whale	Other Whale	Porpoise	Dolphin
Sperm Whale Cry	17	0	0	3
Other Whale	0	16	4	3
Porpoise	0	2	14	1
Dolphin	3	2	2	13

Table 12. Confusion matrix for biological data

The continuous wavelet transform with a one sided Gabor wavelet was also used for this data set. The adaptive energy window features were extracted for a 43% correct classification.

Comparison was made between the continuous wavelet transform (CWT) and the short-time Fourier transform (STFT) in classifying the first three classes of this biologics data set. The CWT scales and STFT frequency bins were chosen using three techniques. These are an adaptive technique which centers 10 logithmically spaced scales on the peak of the energy distribution, a technique which matches the scales to the cumulative energy distribution and one which uses 11 fixed logirithmically spaced scales. The classification results in terms of misses are summarized Table 13 below [18].

If we just focus on the results using CART with linear combination splits, the two CWT techniques using adaptive scales clearly outperform the CWT with fixed log scales. These adaptive CWT techniques also outperform all of the STFT techniques which produced comparable results.

Transform: CWT		
	Scale: Adaptive Energy Window with Adaptive Wavelets	
	CART Single Var Split:	1/60
	CART Linear Var Split:	1/60
	PNN:	5/60
	Scale: Cumulative Energy	
	CART Single Var Split:	10/60
	CART Linear Var Split:	1/60
	PNN:	8/60
	Scale: Fixed Log Scale	
	CART Single Var Split:	5/60
	CART Linear Var Split:	8/60
	PNN:	1/60
Transform: STFT		
	Scale: Adaptive Energy Window with Adaptive Wavelets	
	CART Single Var Split:	5/60
	CART: Linear Variable Split:	5/60
	PNN:	5/60
	Scale: Cumulative Energy	
	CART Single Var Split:	5/60
	CART Linear Var Split:	6/60
	PNN:	4/60
	Scale: Fixed Log Scale	
	CART Single Var Split:	5/60
	CART Linear Var Split:	6/60
	PNN:	4/60

Table 13. Classification results of CWT and STFT based methods on Navy biologics data

7.2.3. Analysis of NUWC Classified Transient Databases

We have processed the Navy Transient Database using the Continuous Wavelet transform and the Short-Time Fourier transform both with moment features. These results include three signal classes from the dataset. (The actual class designations are secret or at least sensitive information. The classes were selected because of their frequency of occurrence and relevance to the passive transient detection problem.) The classifier was trained on over 40 events per class and tested on 20 events per class. The CWT and STFT classifiers both performed very well considering the differences between various elements within each class. The confusion matrices are shown in

Table 14. The classes are made up of signals from different environments and a range of signal-

Continuous Wavelet Transform with Moment Features
CART: Linear Variable Split

Misses: 5/60

		True Class		
		A	B	C
	A	20	0	0
Labeled Class	B	0	19	4
	C	0	1	16

Short-time Fourier Transform with Moment Features
CART: Linear Variable Split

Misses: 4/60

		True Class		
		A	B	C
	A	20	0	0
Labeled Class	B	0	18	2
	C	0	2	18

Table 14. Confusion matrices for NUWC classified transient databases

to-noise ratios. However, the SNR is generally high and the between class differences are large enough that these signals do not provide a rigorous comparison of the techniques. As was found in the synthetic signal case, both the CWT and STFT performed comparably at high SNR. We need to add additional noise to these signals to judge the relative performance of the CWT and the STFT.

7.2.4. Analysis of Synthetic Generic Transient Databases

We have conducted both the Comparative Tests of "Between-Class" Identification and the Comparative Tests of "Within-Class" Identification of generic transients using the Wave Packet (WP) [19, 20] based classifier, the Continuous Wavelet Transform (CWT) based classifier, and the STFT based classifier. The following sections detail the results obtained.

7.2.4.1. "Between-Class" Identification Comparative Tests

We have completed the "between-class" identification comparative tests of the WP approach against the CWT based classifier using Morlet Wavelets and the STFT based classifier. These tests

were conducted using a data set consisting of four types of generic transients described in Table 3 and they were performed as a function of signal to noise ratio (SNR). The SNRs we investigated ranged from 50dB to -50dB.

For each of the four types of generic transients, 200 signals were generated using the parameters shown in Table 3. Out of the 200 signals, 180 were randomly selected from each type and used as training samples to train the classifiers. The remaining 20 signals per class (80 signals total) were used as test signals. We have completed the "between-class" identification comparative tests of the WP approach against the CWT based classifier and the STFT based classifier. The number of misses given by each classification scheme as a function of SNR are shown in Table 15. Figure 21 shows the number of misses given by the three approaches plotted against SNR. The results indicated that when the SNR is positive, all three approaches perform extremely well with the WP performing consistently better than the CWT and STFT. When the SNR is negative, the STFT outperforms the other two. In cases where the SNR is worse than -14 dB, all three approaches showed an error of more than 50%.

7.2.4.2. "Within-Class" Identification Comparative Tests

An extended generic transient data set has been generated using Tables 4 to 7 to permit these "within-class" identification tests. For each of the four classes of generic transients, subclasses were generated and used in these tests. They are also being performed as a function of signal to noise ratio (SNR). The SNRs we investigated again ranged from 50dB to -50dB.

To perform the "within-class" identification test for impulsive transients (Type I), 200 signals were generated for each of the four subclasses using the parameters shown in Table 4. Out of the 200 signals, 180 were randomly selected from each subclass and used as training samples to train the classifiers. The remaining 20 signals per subclass (80 signals total) were used as test signals. Table 16. shows the number of misses given by each classification scheme as a function of SNR. Figure 22 shows the number of misses given by the three approaches plotted against SNR. The results indicated that the STFT outperforms the other two approaches in classifying the subclasses within the impulsive transient class. When the SNR is negative, all three approaches showed a "within-class" classification error of more than 50%.

Similarly, 200 signals were generated for each of the four subclasses of ringing transients (Type II) using Table 5. 180 were randomly selected from each subclass and used as training samples to train the classifiers. The remaining 20 signals per subclass (80 signals total) were used as test signals. Table 17. shows the number of misses given by each classification scheme as a function of SNR. Figure 23 shows the number of misses given by the three approaches plotted against SNR. As can be seen, the CWT in general outperforms the STFT and WP based classification schemes in identifying the subclasses within the ringing transient class. When the SNR is worse than -15dB, all three approaches showed a "within-class" classification error of more than 50%.

Similar study was made to the four subclasses of chirp transients (Type III). Table 18. shows the number of misses given by each classification scheme as a function of SNR. Figure 24 shows the number of misses given by the three approaches plotted against SNR. The CWT in general outperforms the STFT and WP based classification schemes in identifying the subclasses within the

Number of Misses

SNR (dB)	CWT	STFT	WP
50	0/80	1/80	0/80
10	2/80	1/80	0/80
8	4/80	2/80	0/80
6	2/80	1/80	0/80
4	1/80	0/80	0/80
2	4/80	1/80	1/80
0	4/80	4/80	3/80
-2	6/80	1/80	2/80
-4	6/80	3/80	4/80
-6	9/80	4/80	8/80
-8	15/80	11/80	25/80
-10	24/80	16/80	19/80
-12	29/80	25/80	47/80
-14	46/80	41/80	51/80
-16	60/80	55/80	57/80
-18	64/80	59/80	63/80
-20	56/80	57/80	61/80
-50	60/80	61/80	57/80

Table 15. "Between-Class" Identification Results

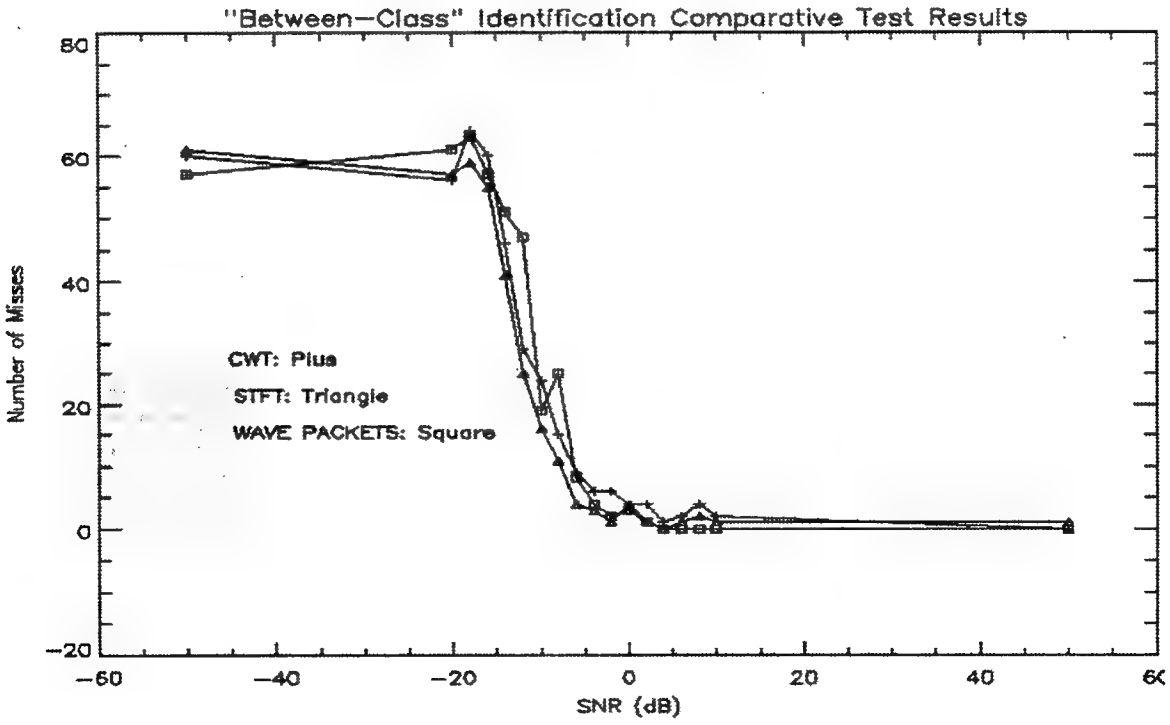

Figure 21. "Between-Class" Identification Results

Number of Misses

SNR (dB)	CWT	STFT	WP
50	1/80	1/80	0/80
25	10/80	4/80	5/80
20	9/80	2/80	8/80
15	21/80	6/80	15/80
10	31/80	13/80	20/80
8	38/80	9/80	34/80
6	34/80	34/80	22/80
4	49/80	27/80	39/80
2	43/80	36/80	37/80
0	53/80	40/80	38/80
-2	53/80	42/80	48/80
-4	52/80	49/80	47/80
-6	60/80	52/80	58/80
-8	62/80	58/80	60/80
-50	58/80	66/80	60/80

Table 16. "Within-Class" Identification Results for Impulsive Transients (Type I)

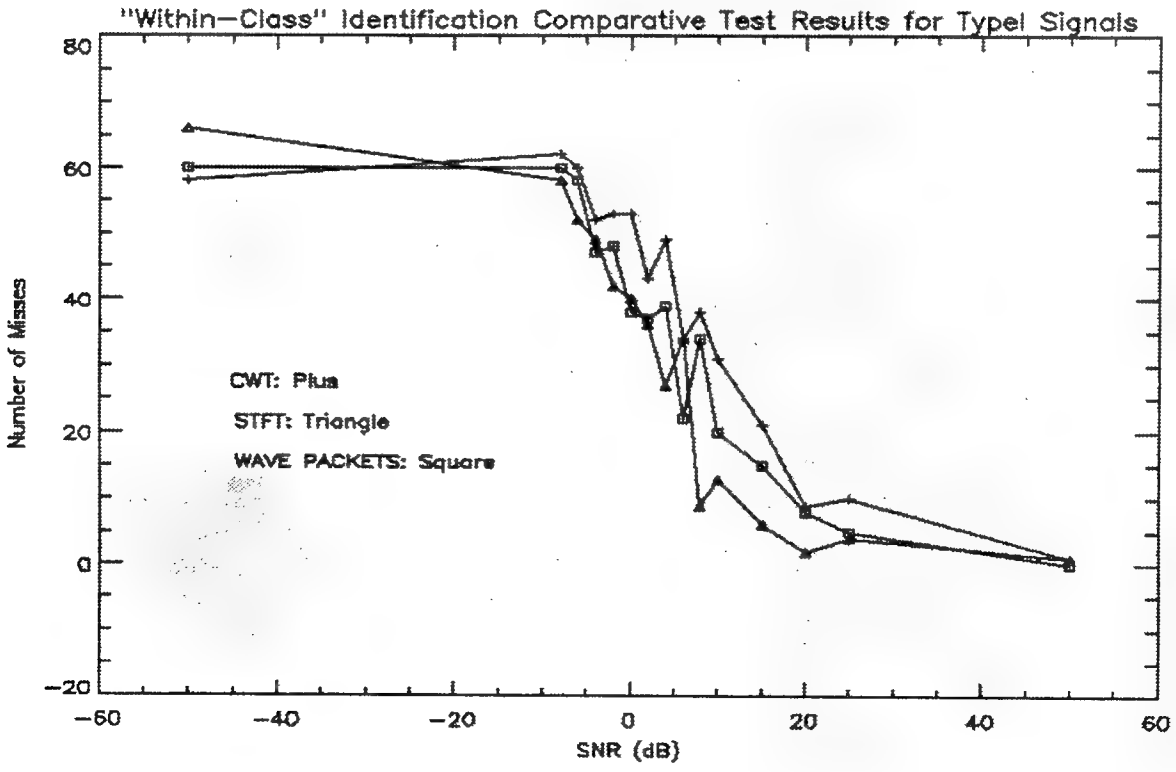

Figure 22. "Within-Class" Identification Results for Impulsive Transients (Type I)

Number of Misses

SNR (dB)	CWT	STFT	WP
50	2/80	0/80	0/80
10	4/80	4/80	9/80
8	2/80	5/80	14/80
6	7/80	6/80	15/80
4	4/80	7/80	15/80
2	6/80	11/80	12/80
0	12/80	14/80	20/80
-2	15/80	19/80	34/80
-4	11/80	18/80	36/80
-6	23/80	36/80	35/80
-8	24/80	39/80	52/80
-10	36/80	50/80	44/80
-15	47/80	57/80	60/80
-25	60/80	60/80	58/80
-50	63/80	67/80	66/80

Table 17. "Within-Class" Identification Results for Ringing Transients (Type II)

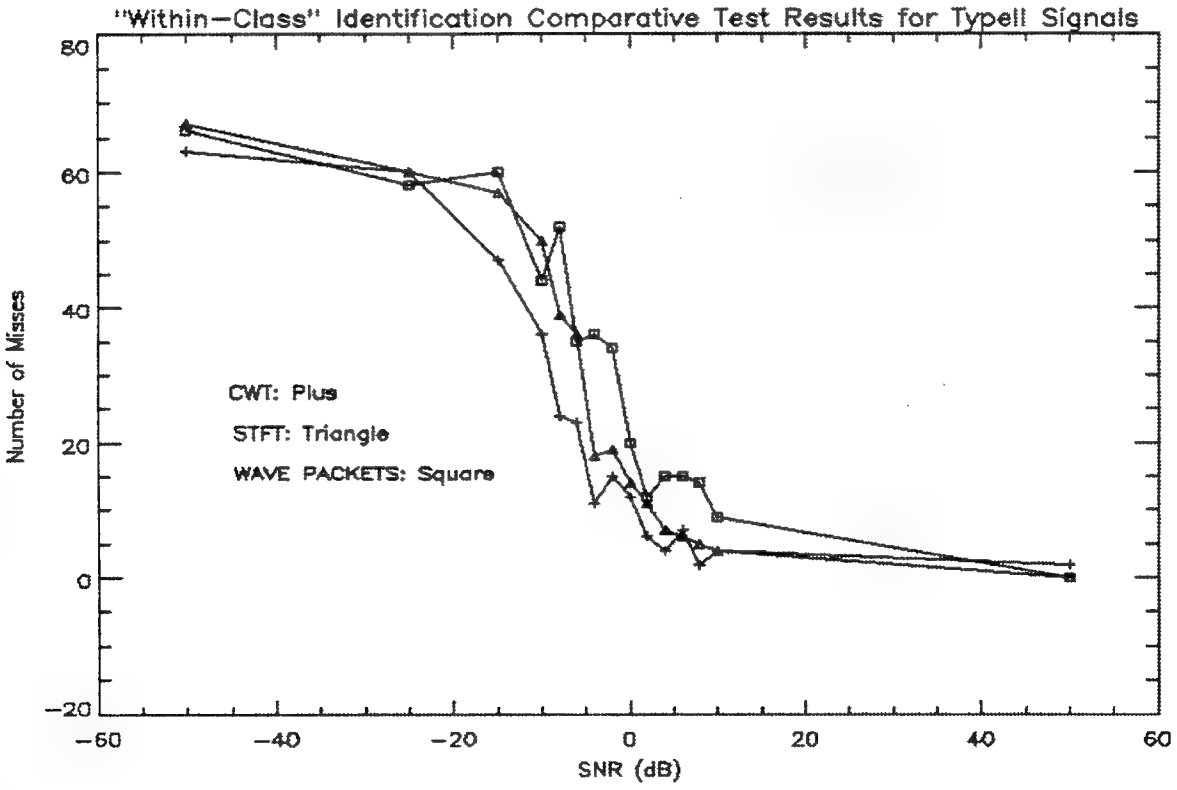

Figure 23. "Within-Class" Identification Results for Ringing Transients (Type II)

Number of Misses

SNR (dB)	CWT	STFT	WP
50	0/80	0/80	3/80
25	0/80	0/80	3/80
20	0/80	3/80	7/80
15	0/80	12/80	6/80
10	1/80	13/80	6/80
8	8/80	23/80	16/80
6	8/80	23/80	16/80
4	10/80	33/80	18/80
2	21/80	35/80	19/80
0	27/80	54/80	16/80
-2	23/80	52/80	27/80
-4	31/80	58/80	24/80
-6	39/80	60/80	39/80
-8	40/80	58/80	41/80
-10	44/80	54/80	55/80
-50	60/80	60/80	57/80

Table 18. "Within-Class" Identification Results for Chirp Transients (Type III)

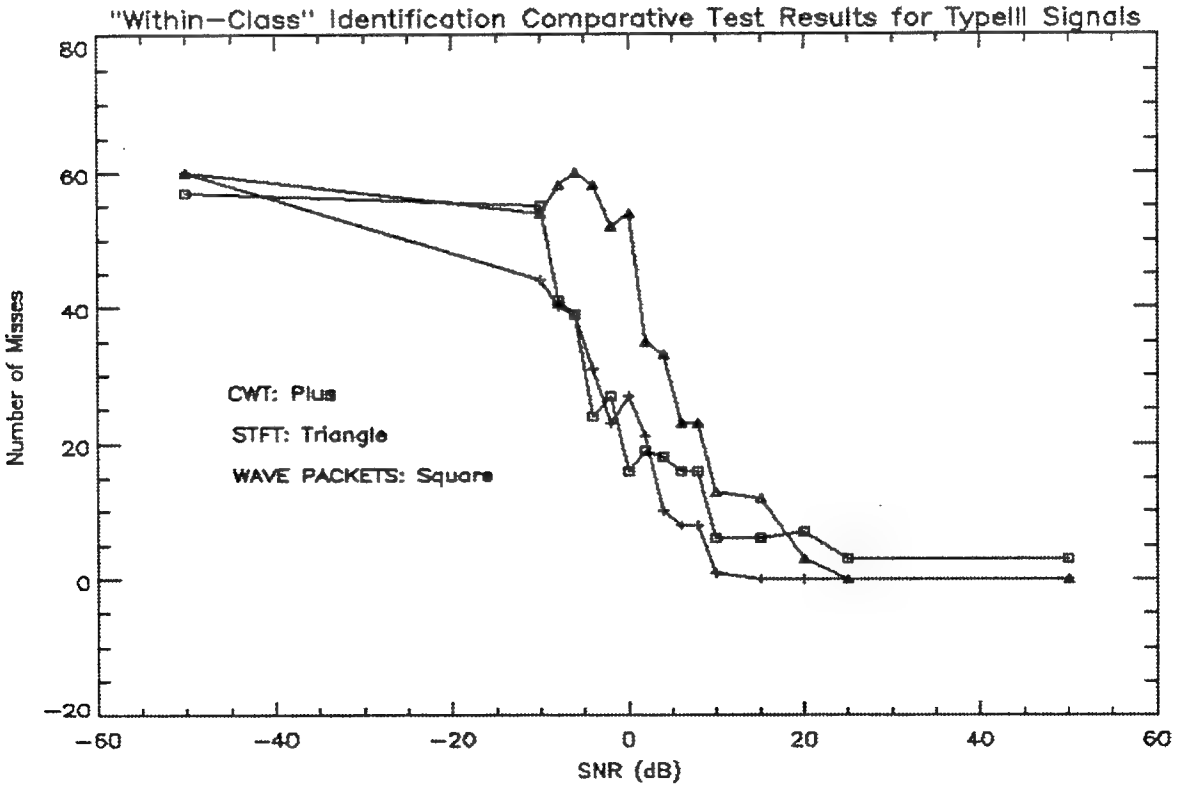

Figure 24. "Within-Class" Identification Results for Chirp Transients (Type III)

chirp transient class. When the SNR is worse than -8dB, all three approaches showed a "within-class" classification error of more than 50%.

8. TECHNOLOGY TRANSFER

8.1. Transfer of Detection and Classification Algorithms to the Multisensor Fusion System

The MSF program is connecting a set of sensor signal processing modules together to provide for increased performance over a single sensor module. Modules include passive narrowband, passive transient, electric field, magnetic field and active sonar processing. The Wavelets program is providing the transient signal processing module as shown in the Figure 25 below. In addition to the software modules shown, data from the MSF Sea Tests is being analyzed. A catalog of several hundred transients has been generated with signals separated by class. These signals were used to train the classifier for the December 22, 1993 demonstration to the ARPA customer.

8.2. Transfer of Wavelets Quicklook Tool to the Multisensor Fusion System

An interactive Wavelets Quicklook Tool has been developed which allows the user to conveniently view and segment the signals for further analysis. This tool has been used extensively in this Contract and has also been transferred to the MSF Program for their use. This tool permits random access of data in huge databases. Various transforms and displays are possible in addition to listening to selected signal segments. This capability allows the extraction of signals of interest and classifying them based on both sound and transform characteristics. Screening and processing of MSF Sea Test data would not have been possible without the wavelet quicklook tool. A snapshot of this tool is given in Figure 26. Some its features include:

1) Interactive graphic display of the signal. User selects a section of the signal using point and click.
2) Separate interactive graphic display of selected portion of the signal. User can scroll the selected segment in either direction in real time.
3) User can perform FFT or STFT on selected segment and view the results as either a 2D, mesh or image type plot.
4) User can listen to selected segment.
5) Signal section information can be saved to a log file for later retrieval by either this tool or the classifier.
6) New signals are graphically selected from a menu of choices.
7) All features are menu selectable.

9. RELATED ACTIVITIES

9.1. Parallel Implementation of Continuous Wavelet Transform

A fast continuous wavelet transform was developed using concepts similar to those detailed in

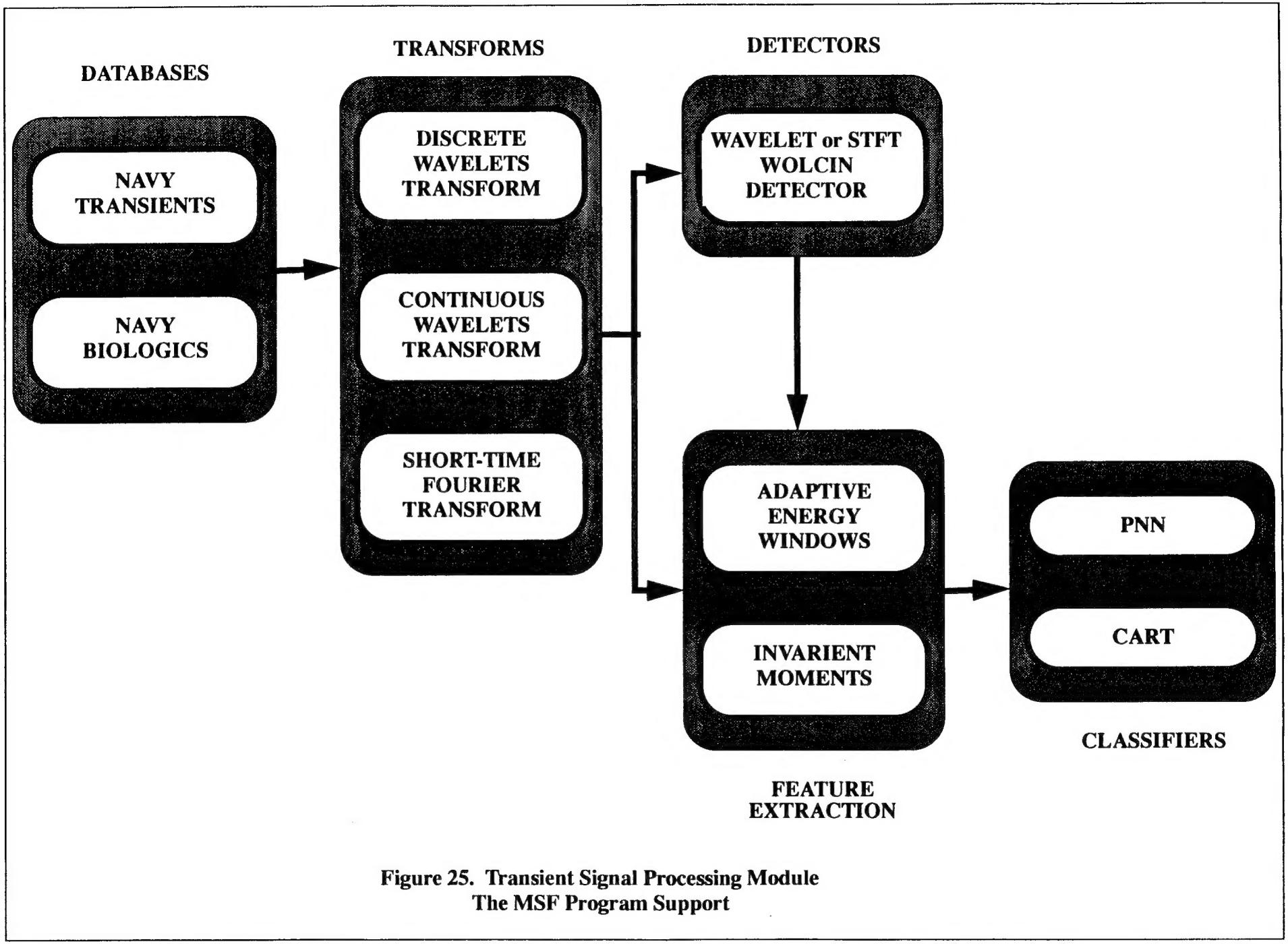

Figure 25. Transient Signal Processing Module
The MSF Program Support

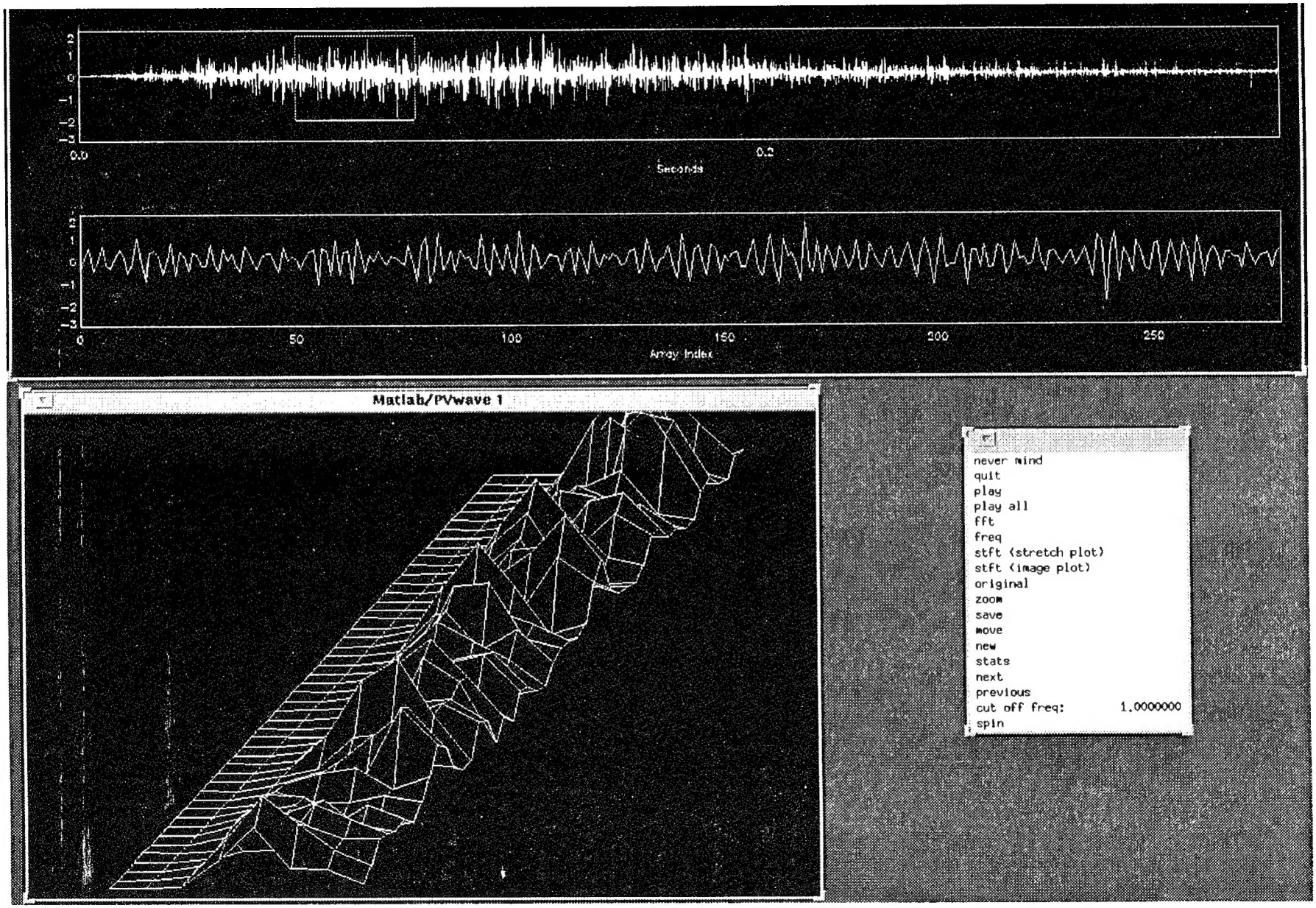

Figure 26. Snapshot of Wavelet Quicklook Tool

[14]. Under a Lockheed Independent Research project on parallel computation this algorithm was implemented on a Wavetracer Zephyr SIMD computer. This machine has 8192 processor elements. Each 9 MHz processor has 256 bytes of internal memory. Timing benchmarks of the Wavetracer results were compared to a Sparc 2 The Sparc 2 performs at 26000 kWhetstones. (Whetstones measure single precision floating point processing power. An 8 MHz 8088/8087 IBM PC performs at 140 kWhetstones. The Sparc 2 is approximately 100 times as powerful as the basic Wavetracer processing element.) Table 19 shows the effective speed up obtained using the Wavetracer.

Signal Size	Sparc 2	Wavetracer	Speed-up factor
256	4.53	1.42	3.19
512	9.12	2.69	3.39
1024	21.95	4.91	4.47
2048	44.90	9.49	4.73

Table 19. Timing Benchmarks

9. 2. Classification of Active Sonar Signals

Classification of Active Sonar Signals is being performed under an Independent Research project in the Lockheed Research & Development Division. Comparative tests were performed between a discrete wavelet transform (furnished by the Wavelet Program) approach and the short-time Fourier transform. Features were extracted using fixed position energy windows. The energy windows were fixed in position because the characteristics of the transmitted active signal is known and the windows can be positioned to serve as "matched filters" for the expected returns. Significantly better results were obtained using the wavelet transform.

10. REFERENCES

1. R. C. Olson, "An overview of underwater acoustic transient signal processing", U.S.Navy Journal of Underwater Acoustics, Vol. 40, no. 4, pp. 717-751, Oct, 1990.
2. I. Daubechies, "Orthonormal bases of compactly supported wavelets", Comm. in Pure and Applied Math., Vol. 41m no. 7, pp. 909-996, 1988.
3. O. Rioul and M. Vetterli, "Wavelet and Signal Processing," IEEE SP Mag. pp. 14-35, Oct. 1991.
4. Ramesh Gopinath, "State Space Approach to Multiplicity M Wavelets", Rice Technical Report CMU-TR-9119, Submitted to IEEE Trans. SP.
5. J. B. Allen and L. R. Rabiner, "A unified approach to short-time Fourier analysis and synthesis", Proc of the IEEE, Vol. 65, no. 11, pp.1558-1564, Nov. 1977.
6. W. Martin and P. Flandrin, "Wigner-Ville spectral analysis of non-stationary processes", IEEE Trans. on Acoustics, Speech and Signal Processing, Vol. 33, no. 6, pp. 1461-1470, Dec. 1985.
7. L. Cohen, "Time-Frequency Distributions - A Review", Proc of the IEEE, Vol. 77, no. 7, pp.

941-981, July 1989.
8. B. Friedlander and B. Porat, "Detection of transient signals by the Gabor representation", IEEE Trans. Acoust., Speech and Signal Proc., Vol. 37, no. 2, pp. 169-180, 1989.
9. R. A. Gopinath and C. S. Burrus, "Efficient Computation of the Wavelet Transform", in Proc. IEE Int. Conf. Acoust., Speech, Signal Processing, Albuquerque, NM, Apr. 3-6, 1990, pp. 1599-1601.
10. R. S. Loe, K. Jung, K. Anderson and S. Shen, "Wavelet Subband Features", Proc. IEEE Symposium on Signal Processing, Victoria, Canada, pp. 517-520, Oct. 4-6, 1992.
11. K. Fukunaga, Introduction to Statistical Pattern Recognition, Academic Press, New York 1972.
12. K. Lashkari, B. Friedlander, J. Abel, B. McQuiston, "Classification of Transient Signals", IEEE Proc. Conf. Acoustics, Speech, Sig. pp. 2689-2692, Sept. 1988.
13. F. Lari and A. Zakhor, "Automatic Classification of Active Sonar Data Using Time-Frequency Transforms", Proceedings IEEE-SP Int. Symp. on Time-Frequency and Time-Scale Analysis, pp. 21-24, Victoria, Canada, Oct. 5, 1992.
14. D. F. Specht, "Probabilistic Neural Networks", Neural Networks Vol. 3, pp. 109-118, 1990.
15. D. F. Specht, "Enhancements to Probabilistic Neural Networks", in Proc. IEEE Int. Conf. Neural Networks, Baltimore, MD, June 7-11, 1992.
16. L. Breiman, J. H. Friedman, R. A. Olshen, C. J. Stone, Classification and Regression Trees, Wadsworth International Group Inc., Belmont, CA, 1984.
17. R. S. Loe, K. Jung, K. Anderson, A. Abatzoglou, J. Regan, H. Arnold and W. Lawton, "Status Report on Wavelets in Signal Detection and Identification", Proc. IEEE Sixth SP Workshop on Statistical Signal & Array Processing, Victoria, Canada, Oct. 5-7, 1992.
18. R. S. Loe, K. Jung, and K. Anderson, "Comparative Analysis Results for Underwater Transient Classification" Proc. SPIE Wavelet Applications, pp. 815-823, Orlando, FL, April 5-8, 1994.
19. M. V. Wickerhauser and R. R. Coifman, "Acoustic Signal Compression with Wave Packets", preprint Yale University, 1989.
20. R. E. Learned, W. C. Karl and A. S. Wilsky, "Wavepackrt Based Transient Signal Classification", in Proc. IEEE Sixth SP Workshop on Statistical Signal & Array Processing, Victoria, Canada, Oct. 5-7, 1992.